Voltammetric characterization of soluble polyacetylene derivatives obtained from the ring-opening metathesis polymerization (ROMP) of substituted cyclooctatetraenes

ARTICLE *in* JOURNAL OF THE AMERICAN CHEMICAL SOCIETY · JUNE 1993

Impact Factor: 12.11 · DOI: 10.1021/ja00064a035

OFFICE OF NAVAL RESEARCH

Grant No.:N00014-91-J-1303

R&T Code: 4132019

Technical Report No.: 2

Voltammetric Characterization of Soluble Polyacetylene Derivatives Obtained from the Ring-Opening Metathesis Polymerization (ROMP) of Substituted Cyclooctatetraenes

by

Thomas H. Jozefiak, Eric J. Ginsburg, Christopher B. Gorman,
Robert H. Grubbs and Nathan S. Lewis

Prepared for Publication in

J. Am. Chem. Soc.

Division of Chemistry and Chemical Engineering
California Institute of Technology
Pasadena, CA 91125

Friday, January 15, 1993

REPORT DOCUMENTATION PAGE

Form Approved OMB No. 0704-0188

1. AGENCY USE ONLY (*leave blank*)	2. REPORT DATE	3. REPORT TYPE AND DATES COVERED
	1/15/93	Technical Report 1/1/92 - 12/31/92

4. TITLE AND SUBTITLE

Voltammetric Characterization of Soluble Polyacetylene Derivatives Obtained from the Ring-Opening Metathesis Polymerization (ROMP) of Substituted Cyclooctatetraenes

5. FUNDING NUMBERS

N00014-91-J-1303

6. AUTHOR(S)

Thomas H. Jozefiak, Eric J. Ginsburg, Christopher B. Gorman, Robert H. Grubbs and Nathan S. Lewis

7. PERFORMING ORGANIZATION NAMES (S) AND ADDRESS(ES)

California Institute of Technology
Mail Code: 164-30
Pasadena, CA 91125 USA

8. PERFORMING ORGANIZATION REPORT NUMBER

2

9. SPONSORING/ MONITORING AGENCY NAME(S) AND ADDRESSES(ES)

Office of Naval Research
800 North Quincy Street
Arlington, VA 22217-5000

10. SPONSORING/ MONITORING AGENCY REPORT NUMBER

11. SUPPLEMENTARY NOTES

J. Am. Chem. Soc., in press.

12a. DISTRIBUTION/ AVAILABILITY STATEMENT

unlimited

12b. DISTRIBUTION CODE

13. ABSTRACT (*Maximum 200 words*)

High molecular weight amorphous, partially substituted polyacetylenes (poly-RCOT) have been prepared using the ring-opening metathesis polymerization of substituted cyclooctetraenes. Spin-cast films of these polymers yielded unusually sharp, well-defined, reversible electrochemistry for oxidative and reductive doping processes. As the substituent on the polymer chain was varied (R=alkyl, *tert*-butoxy, trimethylsilyl, and *p*-X-phenyl) potentials for oxidative and reductive doping changed by 0.3 V. In addition, the separation between the oxidative and reductive doping processes varied from 1.66 to > 2.0 V. Coulometry suggested that the reversible doping step represented a transfer of 1 electron for every 13-15 double bonds of the polymers. In contrast the electrochemistry of predominantly-*cis* poly-RCOT films was irreversible, and indicated the presence of an electrochemical *cis-trans* isomerization on the first voltammetric sweep through either reductive or oxidative doping. Spectroelectrochemical studies indicated that the electrochemically doped poly-RCOT materials (R=*sec*-butyl, $(CH_3)_3Si$ possessed mid-gap transitions at energies of 0.8-0.9 eV. The redox chemistry is soluble poly-RCOT (R=*sec*-butyl, $(CH_3)_3Si$) species in CH_2Cl_2 solution was also investigate. Voltammetric studies showed that both the reductive and oxidative doping processes were chemically irreversible, and indicated that the dissolved polymers were electroactive over a wide range of potentials.

14. SUBJECT TERMS	15. NUMBER OF PAGES
	16. PRICE CODE

17. SECURITY CLAIFFICATION OF REPORT	18. SECURITY CLASSIFICATION OF THIS PAGE	19. SECURITY CLASSIFICATION OF ABSTRACT	20. LIMITATION OF ABSTRACT
unclassified	unclassified	unclassified	UL

Voltammetric Characterization of Soluble Polyacetylene Derivatives Obtained from the Ring-Opening Metathesis Polymerization (ROMP) of Substituted Cyclooctatetraenes

Thomas H. Jozefiak, Eric J. Ginsburg, Chris B. Gorman, Robert H. Grubbs*, and Nathan S. Lewis*

Contribution No. 8645 from the Arnold and Mabel Beckman Laboratory of Chemical Synthesis and the Arthur A. Noyes Laboratory of Chemical Physics
The Division of Chemistry and Chemical Engineering
California Institute of Technology
Pasadena, CA 91125

ABSTRACT

High molecular weight, amorphous, partially substituted polyacetylenes (poly-RCOT) have been prepared using the ring-opening metathesis polymerization of substituted cyclooctetraenes. Spin-cast films of these polymers yielded unusually sharp, well-defined, reversible electrochemistry for oxidative and reductive doping processes. As the substituent on the polymer chain was varied (R = alkyl, *tert*-butoxy, trimethylsilyl, and *p*-X-phenyl), the potentials for oxidative and reductive doping changed by 0.3 V. In addition, the separation between the oxidative and reductive doping processes varied from 1.66 V to > 2.0 V. Coulometry suggested that the reversible doping step represented a transfer of 1 electron for every 13-15 double bonds of the polymer. In contrast, the electrochemistry of predominantly- *cis* poly-RCOT films was irreversible, and indicated the presence of an electrochemical *cis-trans* isomerization on the first voltammetric sweep through either reductive or oxidative doping. Spectroelectrochemical studies indicated that the electrochemically doped poly-RCOT materials (R=*sec*-butyl, $(CH_3)_3Si$) possessed mid-gap transitions at energies of 0.8-0.9 eV. The redox chemistry of the soluble, poly-RCOT (R=*sec*-butyl, $(CH_3)_3Si$) species in CH_2Cl_2 solution was also investigated. Voltammetric studies showed that both the reductive and oxidative doping processes were

chemically irreversible, and indicated that the dissolved polymers were electroactive over a wide range of potentials.

I. INTRODUCTION

There is intense interest in the synthesis of highly conjugated organic polymers.[1-3] Most recently, attention has focused on the synthesis of conjugated polymers that are soluble in common organic solvents.[4-6] Processable, soluble, electrically conducting polymers might be useful in a variety of novel optoelectronic devices,[7-10] such as polymer-based field effect transistors and polymer-based Schottky diodes.[11-13] However, at present, very few reactions produce polymers with the desired combination of chemical and electronic properties.

One approach to this problem involves the synthesis of substituted polypyrrole and polythiophene derivatives.[14-17] In principle, the polymerization of substituted acetylenes should provide an even simpler synthetic route to processable, conjugated polymers. Such polyenes often are soluble, but generally do not have long π-conjugation lengths.[18-20] To address this issue, Grubbs and co-workers have recently prepared a family of substituted poly-cyclooctatetraenes (poly-RCOT) using a ring-opening metathesis polymerization (ROMP) route (Scheme 1).[21-26] These polyacetylene-like polymers exhibit the desired combination of solubility in organic solvents and long π-conjugation lengths. Additionally, they can be doped to yield polymers with high electrical conductivities. This set of materials is the topic of the spectral and electrochemical studies reported in this work.

One of the desirable features of the poly-RCOTs is the relatively large average distance between substituent groups (*i.e.*, one substituent per eight chain carbons). For example, in poly-*sec*-butylCOT and poly-$(CH_3)_3$SiCOT, the polymer is soluble even in the predominantly-*trans* configuration, yet the steric hindrance is not sufficient to impede extensive planarity between units in the polymer chain. The factors that influence this solubility vs. conjugation length tradeoff have been discussed elsewhere,[22,23,27] and are not the major topic of this investigation. However, the availability of this new class of polymers provides an opportunity to investigate several important questions regarding the thermodynamics and electronic structure of substituted conducting polymer systems. Thus, the work described below is focused on the electrochemistry, spectroelectrochemistry, and electronic structure of these unique materials.

One of the key unanswered questions for conducting polymer systems is how the electrochemistry and electronic structure of polymer films differ from that of polymers in solution.[28-31] Variations in the interactions between the polymer chains, and the restricted conformational mobility of polymer chains in the solid state, could both produce differences between polymer films and solutions of polymers. The availability of soluble polyacetylene derivatives presents an opportunity to explore these questions in detail. Recent spectroscopic studies of soluble polythiophenes have reported optical transitions that are similar to those of bulk polythiophenes.[32] However, in the case of poly-RCOTs, we have obtained evidence that the analogy between dissolved polymer strands and polymer films is not general. In particular, we have observed that soluble poly-RCOTs show a voltammetric response which differs from that of thin poly-RCOT films.

Another issue of interest is how closely the physical and electronic properties of poly-RCOTs resemble those of polyacetylene. Although the structures of poly-RCOTs are closely related to substituted acetylene polymers, it is not obvious that the two different polymerization methods will yield materials with comparable physical and electronic characteristics. Prior optical studies of poly-RCOT systems have shown similar electronic absorption bands to those observed in polyacetylene.[33] In addition, oxidatively doped poly-RCOT films have exhibited high electrical conductivities, with values in the range of 0.03-50 S-cm.[24] Notably, these values are only 1 to 2 orders of magnitude below the highest electrical conductivites reported for polyacetylenes. At present, however, no other data are available to provide a basis for comparison of these materials.

The electronic structure of poly-RCOT films is also of interest with regard to polymer-based optoelectronic devices and chemical sensors. To vary the solubility, optical, and electronic properties of conducting polymers, electron-donating or electron-withdrawing substituents have often been introduced onto the polymer backbone. In this strategy, both steric and electronic effects of the substituent are expected to be important in determining the energetics of polymer doping.[3, 21-26] This type of approach has been used successfully to modify the properties of polypyrroles and polythiophenes. However, it is not yet known whether the introduction of

substituents will significantly affect the doping properties of poly-RCOTs. The desired information can be obtained from the electronic and electrochemical measurements reported herein.

II. EXPERIMENTAL

A. Materials

Acetonitrile (Aldrich HPLC grade) was distilled from CaH_2, and was stored in N_2(g) over 3 Å molecular sieves. Methylene chloride (Burdick and Jackson high purity grade) was distilled from P_2O_5, and tetrahydrofuran (THF) was vacuum transferred from a solution of the potassium benzophenone dianion. Electrometric grade tetra-(*n*-butyl)-ammonium tetrafluoroborate ($TBABF_4$) (recrystallized from 3:1 by volume water:methanol), tetraethylammonium tetrafluoroborate ($TEABF_4$) (recrystallized from 5:1 by volume ethyl acetate:pentane), and tetramethylammonium tetrafluoroborate ($TMABF_4$) (recrystallized from acetone) were used as electrolytes, and were purchased from Southwestern Analytical Chemicals Inc.. After recrystallization, these electrolytes were dried by heating to 80°C for >36 hours in vacuo. All solvents and electrolytes were stored in a Vacuum Atmospheres dry box that was filled with N_2(g).

Monosubstituted COT monomers[27] and the tungsten alkylidene catalyst[34] were synthesized as reported previously. The substituted COT monomers, which were mildly air sensitive, were purified by distillation at reduced pressure. The monomers were then stored in a dry box at -20 °C. The neat RCOT monomers were then polymerized in a dry nitrogen atmosphere, as described previously.[21,23,26] In this work, the tungsten carbene complex $W(CHAr)(NPh)(OR_f)_2(THF)$, with Ar = *o*-$C_6H_4$-$OCH_3$ and OR_f = $OC(CH_3)(CF_3)_2$ was used as the ROMP catalyst.[35] The resulting polymers were treated as air- and moisture-sensitive compounds.

For quantitative electrochemical experiments, special care was taken to end-cap the polymers. Impurities were washed away from this end-capped material, and volatiles were then pumped off the purified polymer. In a typical procedure (performed in the dry box), 10.3 mg (1.24×10^{-5} mol) of the tungsten carbene metathesis catalyst was dissolved in a small volume (100 µL) of olefin-free pentane. This solution was then mixed with neat *sec*-butylCOT (0.300 g, 1.87×10^{-3} mol). Within minutes at ambient temperature, the mixture became viscous, and its color

changed from orange-yellow to dark brown-red. After two hours, the mixture had solidified, and the dark brown-red polymer film was then manually peeled from the reaction vessel. This procedure produced one continuous piece of polymer film. To end-cap the polymer, the film was dissolved in a benzene solution (20 mL) that contained a small amount of benzaldehyde (50 μL). After stirring for one hour, the solvent and end-capping agent were removed under vacuum. In an inert atmosphere, the resulting polymer film was then washed repeatedly with pentane and methanol.

Except where otherwise specified, the purified polymer film was then deliberately converted to the predominantly-*trans* configuration. To achieve this conversion, the polymer film was dissolved in tetrahydrofuran (1-2 mg polymer/mL THF solution) and was poured into a Pyrex tube sealed with a Teflon screw cap. The solution was maintained at 0 °C and was illuminated, through a Pyrex filter, by the light from a 350 watt medium-pressure Hanovia mercury lamp. After approximately two hours of illumination, the visible absorption spectrum of the polymer had stopped changing, and displayed a single peak with $\lambda_{max} = 555$ nm. At this point, the isomerization was judged to be complete. In some instances, the isomerization reaction was allowed to occur spontaneously by stirring THF/polymer solutions for 5-10 days in the dry box. After either isomerization procedure, the solvent was then removed from the polymer solution by pumping under vacuum. Before use, the dry film was maintained for at least 3 days under a vacuum of 1 mTorr.

B. Electrochemical Measurements

All electrochemical measurements were performed under $N_2(g)$ in a Vacuum Atmospheres dry box. Cyclic voltammetry was performed using a 3-electrode configuration in a 1-compartment cell. A typical reference electrode was a silver wire immersed into a CH_3CN-0.1 M $TBABF_4$-$AgNO_3$ solution, and contact between the reference compartment and working electrode compartment was achieved with a Vycor glass junction. The reference electrode was regularly calibrated against the ferrocene (Fc)/ferrocenium couple (CH_3CN, 0.1 M $TBABF_4$). For consistency between different experiments, all potentials were converted to the standard calomel

electrode (SCE) scale using a value of $E^{o'}(Fc^+/Fc) = 0.420$ V vs. SCE. Electrochemical measurements were performed using a Princeton Applied Research Model 173 potentiostat, Model 175 voltage programmer, and Model 179 digital coulometer.

Polymer-modified electrodes were prepared by depositing several microliters of a polymer/THF solution (0.3-0.5 mg polymer/mL THF) onto a 5.5 mm diameter glassy carbon disc. The THF was then allowed to evaporate, leaving a thin polymer film (0.2-0.5 μm in thickness, as measured by profilometry) for use in electrochemical experiments. Unless otherwise stated, the solutions were made with polymer that had been isomerized to the thermodynamically preferred, predominantly-*trans* configuration.

Microelectrode voltammetry was carried out using a platinum disc microelectrode of radius 4.23 μm (Bioanalytical Systems Inc.). These measurements were performed in the dry box using shielded cables. For measurement of the small currents obtained from microelectrodes, a Keithley Model 427 current amplifier was used in conjunction with the Princeton Applied Research Model 173/175 potentiostat/programmer.

Spectroelectrochemistry was performed in a homemade 3-compartment cell. In this cell, electrochemistry was performed in a 3-electrode configuration, with a fritted disk isolating the auxiliary electrode from the main cell compartment. The optically transparent electrode was a glass slide that had been coated with In_2O_3. To complete the spectroelectrochemical cell, this slide was then inserted into a standard 1.00-cm path length optical cell. For visible spectroscopy, the entire assembly was then mounted into a Hewlett Packard Model 8452 diode array spectrometer. For spectroscopy in the near infrared region of the spectrum, the cell was inserted into a Cary-14 spectrometer that had been modified with an Olis-4300S System.

Before spectroelectrochemistry, polymer films were cast or spin-coated onto the transparent In_2O_3 electrode. They were then characterized electrochemically before use in the optical experiments. After a potential step, optical spectra were only recorded after the absorption data were independent of time.

Electrochemical measurements on polymer films were typically performed in acetonitrile, in the presence of either $TMABF_4$ or $TEABF_4$ as supporting electrolyte. Unexpectedly, when the electrolyte cation was lithium or potassium (for example, when lithium perchlorate or potassium triflate were the electrolytes), a single cathodic doping cycle resulted in loss of electroactivity. This is not readily understood at present, because polyacetylene films have been reductively doped in the presence of alkali metal cations.[36] However, in the presence of K^+ or Li^+, the electrochemistry of all poly-RCOT films showed similar, irreversible electrochemistry at negative potentials. Therefore, all of the quantitative results reported below were obtained in solutions where tetraalkylammonium salts were the electrolytes. In these solutions, the voltammetry was reproducible from scan to scan, with little chemical degradation of the polymer films during the electrochemical experiments.

Charge vs. potential data were collected for the oxidation and reduction of poly-*sec*-butylCOT and poly-$(CH_3)_3$SiCOT. Several assumptions were required, however, in order to extract the faradaic charge from the total measured charge. For the fully doped film, the rate of capacitive charging was taken to be the constant rate (dQ_{cap}/dV) in the plateau region of the wave. The capacitance of partially doped films was then assumed to be linearly proportional to the charge passed during doping. Once the charging rate for the fully oxidized film was determined, the Q vs. V curve was broken down into small voltage increments (dV). The weighted capacitive charge was then subtracted from the total observed charge in each interval. The adjusted charge values for each voltage interval were then summed, and these values yielded a Q vs. V curve for the faradaic component of the charge. This calculation was performed using a standard spreadsheet program. Although the shape of the Q vs. V curve was affected by the voltage sweep rate, the calculated faradaic Q vs. V data were found to be independent of sweep rate for values $\leq$ 50 mV/sec. At higher sweep rates ($\geq$100 mV/sec), the distinction between the peak and plateau regions in the Q vs. V data was less clear. The simple charging model was therefore not used to analyze the coulometry under these conditions.

III. RESULTS

A. Electrochemistry of poly-RCOT Films

1. Voltammetry of Thin Films

All poly-RCOT materials were found to be soluble in nonpolar solvents such as methylene chloride, toluene, and tetrahydrofuran (THF). Due to this solubility, thin polymer films could be prepared using standard spin-coating methods. Generally, THF was used as the solvent for the spin-casting process. Electrochemistry on these polymer-modified electrodes was then performed in CH_3CN-$TMABF_4$, where the polymer films were insoluble. Figure 1 displays an example of the voltammetry exhibited by this type of polymer-modified electrode.

All poly-RCOT films exhibited prominent, well-defined faradaic currents for both the oxidative and reductive doping processes. As expected for a surface-attached voltammetric wave, the peak currents for both the oxidative and reductive doping processes increased linearly with increasing sweep rate. Additionally, for both types of doping, the voltammetric peaks were extremely sharp. In fact, typical full widths at half maximum were 50±5 mV for the charging waves and 80±5 mV for the discharging waves (at 20 mV/sec in CH_3CN-$TMABF_4$ electrolyte).

At sweep rates ≤ 50 mV/sec, the cathodic (E_{pc}) and anodic (E_{pa}) peak potentials were unusually close together for a conducting polymer film. The charge/discharge peak separation increased with increasing scan rates, as typically found for most surface-attached electroactive films. However, even at the faster sweep rates, the waves for poly-RCOT films were unusually closely spaced, given prior literature results for the voltammetry of other conducting polymers.[37,38]

This combination of sharp peaks and small separations between E_{pa} and E_{pc} implies that the voltammetry can yield an excellent estimate of $E^{o'}$ for the doping process. Table 1 lists the apparent formal potentials, $((E_{pc}+E_{pa})/2)$, obtained from the voltammetric data. Within the group of RCOT polymers, the variation of $E^{o'}$ for the oxidative doping process was 0.28 V. For the same group of polymers, $E^{o'}$ varied by 0.37 V for the reductive doping process. This variation in

$E^{o'}$ reflects the combined steric and electronic influence of the substituent on the π-backbone (*cf.* section **IV.A**).

Another important feature of the voltammograms is the separation between $E^{o'}$ values for the oxidative and reductive doping processes. This separation varied from 1.66 V to >2.0 V in the poly-RCOT series. Within a comparable series of poly-RCOT materials, this separation correlated well with optical measurements of the conjugation length (Table 1).

As expected, the kinetics of charge propagation were a function of the supporting electrolyte. In fact, the reductive charge/discharge wave was severely distorted when the supporting electrolyte was $TBABF_4$ (charging peak full width at half maximum $\approx$ 0.20 V, and $E_{pa} - E_{pc} \approx$ 0.20 V). In contrast, for $TMABF_4$, the reductive doping wave was extremely sharp (charging peak width at half height = 40±5 mV, $E_{pa} - E_{pc} <$ 80 mV). With $TEABF_4$ as the electrolyte, the reductive doping wave was of intermediate width. For this reason, $TMABF_4$ was used when measuring $E^{o'}$ for the reductive doping of poly-RCOT films.

2. *Coulometric Data for Doping Processes of Poly-RCOT Films*

Coulometric measurements verified that doping of poly-RCOT films was chemically reversible. For example, for two representative materials (R=*sec*-butyl and R=$(CH_3)_3Si$), most (≈95%) of the charge observed in the doping process was consumed on the subsequent discharge sweep. This behavior was observed for the oxidative and reductive doping processes of the polymers.

For conducting polymers, the doping stoichiometry cannot be obtained directly from coulometric data. In fact, without a simplifying assumption, the total charge in such systems cannot even be separated into faradaic and capacitive components.[39-42] For our polymer-modified electrodes, the rate of charging (dQ/dV) became constant at potentials beyond the peak region of the doping wave (Figure 2). This current was therefore assumed to approximate the charging current of the fully doped film. Consistently, voltammetric cycling in this potential region showed only a broad, flat capacitive current envelope. Furthermore, spectroelectrochemistry *(vide infra)*

showed that potential steps within this region did not result in any change in the visible absorbance spectrum of the doped film.

For electrodes modified with poly-*sec*-butylCOT, this procedure yielded values of 15.5±0.6 double bonds per electron transferred ((C=C)/e$^-$) during oxidative doping and 14.2±0.6 (C=C)/e$^-$ during reductive doping. For poly-$(CH_3)_3$SiCOT, similar values were obtained: 14.3±0.6 (C=C)/e$^-$ during oxidative doping, and 14.0±0.6 (C=C)/e$^-$ during reductive doping. For comparison, polyacetylene has been doped chemically and electrochemically to a stoichiometry of up to 0.1 dopant equivalent per chain carbon, or 5 (C=C)/e$^-$.[43] However, polyacetylene has also been reported to exhibit a broad range of doping stoichiometries. This variation in stoichiometry has been ascribed to variations in the crystalline morphology of the polymer phase.[44] Thus, differences in doping stoichiometry between crystalline polyacetylene and the amorphous poly-RCOT films are not surprising.

3. Electrochemical Stability of Poly-RCOT Films

The electrochemical doping/undoping of poly-RCOT films was generally chemically reversible. However, the charge capacity decreased slightly after prolonged electrochemical charging/discharging. For example, for poly-*sec*-butylCOT, approximately 2% of the charging capacity was lost on each oxidative charge/discharge cycle (for sweep rates <100 mV/sec). The films were more stable during reductive doping, but the charge capacity still decayed significantly after extended potential cycling. Polyacetylene is known to be highly reactive after either *n*- or *p*-type doping;[45,46] thus, the lack of long-term stability of poly-RCOT films is consistent with this reactivity. Despite this lack of long-term stability, reliable, reproducible electrochemical information could be obtained using freshly prepared poly-RCOT films.

At sufficiently positive potentials, all of the poly-RCOT films yielded a distinct, second oxidation process. This second anodic wave consumed much more charge than the initial oxidative process. Additionally, just one potential sweep through this second wave resulted in a total loss of electroactivity (Figure 3). For most poly-RCOT films, this second oxidation process was well separated from the chemically reversible oxidative doping process. However, for poly-*tert*-

butoxyCOT, this separation was only 0.25 V. As discussed below, this voltammetric behavior is consistent with the poor chemical stability of oxidized poly-*tert*-butoxyCOT films.

4. Spectroelectrochemical Characterization of poly-RCOT Films

Electrochemically doped films of poly-*sec*-butylCOT and of poly-$(CH_3)_3$SiCOT were also characterized by optical spectroscopy ($350 < \lambda < 2100$ nm). Oxidative doping (In_2O_3 electrode, $E=(E_{pa}+0.15$ V), CH_3CN-0.1 M $TEABF_4$) resulted in the disappearance of the strong interband transition in the visible region, and produced a strong transition in the near infrared (Figure 4). Reductive doping (In_2O_3 electrode, $E=(E_{pc}-0.20$ V), CH_3CN-0.1 M $TEABF_4$) of these films produced similar spectroscopic changes. The near-IR spectrum obtained after oxidative doping was broader than that observed after reductive doping, but λ_{max} was the same in both cases.

The λ_{max} for electrochemically doped poly-$(CH_3)_3$SiCOT was slightly smaller than λ_{max} for poly-*sec*-butylCOT. Furthermore, the transitions for both of these doped RCOT polymers were at higher energy than the transition in unsubstituted, doped polyacetylene (Table 2). For polyacetylene, intragap transitions are thought to be responsible for the electronic absorption in the near infrared.[33] Our results are also consistent with this interpretation for poly-RCOT films.

In a related experiment, spectral data were obtained as a function of the electrode potential. Figure 5 displays this type of spectroelectrochemical experiment for a poly-*sec*-butylCOT-coated In_2O_3 electrode. As the process proceeded, the intensity of the interband transition decreased, and the near infrared absorption increased (Figure 5). In addition, the interband transition for the neutral polymer exhibited a blue-shift in λ_{max}. This might indicate that polyene segments of longer conjugation lengths were preferentially oxidized. Another possibility, however, is that the blue-shift resulted from movement of the Fermi level in the valence band of the neutral polymer. The Fermi level shift would be more consistent with the electrochemical measurements (*vide infra*), but the preferential oxidation of certain polymer segments cannot be conclusively ruled out at present.

After repeated charge/discharge cycles in CH_3CN, poly-RCOT films became nearly colorless and lost electroactivity. During repeated oxidative charge/discharge cycles, the visible absorption of the neutral poly-RCOT material shifted toward higher energies and lost intensity. The same changes

were seen for the near infrared band of the oxidatively doped film. During repeated reductive charge/discharge cycles, the visible band of the neutral film distorted, and a shoulder appeared on the high energy side of the band. Also, the near infrared band of the reductively doped film lost intensity and shifted slightly to higher energies. After this process, the solution was analyzed optically, but no significant absorption in the visible or near infrared was observed.

5. Electrochemically Induced cis-trans Isomerization of poly-RCOT Films

Although the ROMP synthesis yields predominantly the *cis* isomer of the RCOT polymers, all of the voltammetry described above was performed on films having a predominantly-*trans* configuration. In this section, we describe the electrochemistry and spectroscopy of the as-synthesized, predominantly-*cis* poly-RCOT materials.

Figure 6 displays typical cyclic voltammetric data for a predominantly-*cis* poly-*sec*-butylCOT film. On the first positive-going potential sweep, a new anodic wave appeared. This wave was located at more positive potentials than the reversible oxidative doping process of the predominantly-*trans* film. The first potential sweep in the negative direction yielded similar behavior, except that the new cathodic wave appeared at more negative potentials than the reversible cathodic doping process. Regardless of the initial scan direction, the voltammetry after this first potential sweep was identical to that observed for predominantly-*trans* poly-*sec*-butylCOT. This strongly suggests that *cis-trans* isomerization can be induced through either reduction or oxidation of the as-prepared, predominantly-*cis* RCOT polymers. An analogous doping-induced *cis-trans* isomerization has been observed in the chemical and electrochemical doping of polyacetylene.[47,48]

To provide support for this hypothesis, the electronic spectra of poly-RCOT films were obtained during the initial voltammetric cycles. Prior to electrochemistry, films of predominantly-*cis* poly-$(CH_3)_3$SiCOT displayed λ_{max}=380 nm. However, after a single voltage cycle (at 20 mV/sec) from 0.0 V to +0.8 V and back to 0.0 V, these films exhibited λ_{max} at 540 nm. Alternatively, the same spectrum, with λ_{max}=540 nm, could be produced by a single voltage cycle from -0.4 V to -1.7 V and back to -0.4 V (at 20 mV/sec). Predominantly-*cis* poly-*sec*-butylCOT

behaved similarly, with a single positive or negative voltage sweep producing a change in the visible absorption spectrum of the film. Again the initial spectrum was characteristic of the predominantly-*cis* polymer (λ_{max}=352 nm), and the final spectrum was characteristic of the predominantly-*trans* polymer (λ_{max}= 550 nm). These spectral changes are similar to those observed during the thermal or photochemical *cis-trans* isomerization of poly-RCOT solutions. The spectroelectrochemical data are thus fully consistent with the proposed, electrochemically-induced, *cis-trans* isomerization process.

The anodic isomerization of predominantly-*cis* poly-*sec*-butylCOT was also investigated with coulometry. Even though the polymer isomerized during oxidation, the amount of charge passed in the first positive voltage sweep was within 10% of the charge passed on the subsequent sweep. For example, in Figure 6, the first positive-going sweep between 0.2 V and 0.8 V produced a total anodic charge of 5.02×10^{-4} coulombs. The second positive-going voltage sweep of this same electrode, over the same potential range, displayed an oxidation wave that was characteristic of the predominantly-*trans* polymer. This second voltage scan contained a total anodic charge of 4.50×10^{-4} coulombs. Thus, the amount of charge required to isomerize and dope a predominantly-*cis* poly-RCOT film was nearly equivalent to the charge required to dope the resulting predominantly-*trans* polymer.

Some voltammetric experiments were also performed with partially oxidized, predominantly-*cis* poly-RCOT films. These experiments were designed to test whether the *cis-trans* isomerization of these long chain polyenes was an electrocatalytic process. To perform this experiment, two glassy carbon electrodes were coated with nominally identical amounts of predominantly-*cis* poly-*sec*-butylCOT. One electrode was used to determine the anodic charge passed during isomerization and doping of the film (Figure 7). For the other electrode, the initial potential sweep was reversed when only 22% of the expected anodic charge had passed. A second positive-going voltage sweep on this electrode then displayed a distinct oxidation peak for the predominantly-*trans* poly-*sec*-butylCOT (Figure 7). This peak contained only 27% of the charge expected from the fully isomerized, predominantly-*trans* film. This result indicated that the

electrochemical isomerization was not electrocatalytic. It also indicated that incomplete doping of the predominantly-*cis* film resulted in incomplete isomerization to the predominantly-*trans* polymer.

B. Electrochemistry of poly-RCOT Solutions

1. Voltammetry of Polymer Solutions

Voltammetric studies of poly-RCOT solutions were limited to poly-*sec*-butylCOT and poly-$(CH_3)_3$SiCOT. In CH_3CN, only these two*trans*-poly-RCOTs yielded voltammetric signals above background. Solutions of these two polymers also readily passed material through a filtration membrane with a pore size of 0.45 μm. Other poly-RCOT materials were soluble in their predominantly-*cis* configuration, but aggregated after isomerization to the predominantly-*trans* configuration. The deep blue solutions of these aggregates appeared to be homogeneous to the naked eye, but the polymers did not pass through a filtration membrane with a pore size of 0.45 μm. Furthermore, the filtered solutions yielded no voltammetric response above background for -2.0 V< E < +1.0 V. Thus, only poly-*sec*-butylCOT and poly-$(CH_3)_3$SiCOT provided truly soluble, electroactive polymers.

As displayed in Figure 8, the cyclic voltammetry of CH_2Cl_2-0.1 M $TBABF_4$-predominantly-*trans* poly-*sec*-butylCOT solutions exhibited no obvious current peaks. In particular, the reverse voltage sweep produced small return waves, especially for the reductive charging/discharging process. Similar behavior was observed for solutions of predominantly-*trans* poly-$(CH_3)_3$SiCOT. In these solutions, no return wave was observed for this polymer after either oxidative or reductive doping. In both polymer solutions, no polymeric deposits could be seen visually on the Pt electrode. Additionally, after use in the polymer solutions, these Pt electrodes exhibited no voltammetric peaks in polymer-free CH_2Cl_2-0.1 M $TBABF_4$ solutions.

The voltammetry of these polymer solutions was also investigated using microelectrodes. This method yielded minimal interference from double layer capacitive currents, and also minimized the effects of time-dependent diffusional processes. At a microelectrode, the oxidation of predominantly-*trans* poly-*sec*-butylCOT showed a continuing increase in current during a

positive-going voltage scan (Figure 9). The reductive doping process of this polymer also did not exhibit a well-defined limiting current value. The shape of these voltammetric waves suggested that there was an onset potential for faradaic electrochemistry of the polymer, but that the electrochemistry was spread over a large range of potentials. This behavior was not ascribable to irreversible adsorption of the polymer, because subsequent voltammetric examination of the electrode in CH_2Cl_2-0.1 M $TBABF_4$ solutions yielded no signals above background levels. Similar broad and featureless steady state voltammograms have been observed previously for redox polymers with multiple, highly interacting, redox sites.[49-51] A comparison of Figures 1 and 9 clearly indicates that the voltammetry of dissolved poly-*sec*-butylCOT and poly-$(CH_3)_3$SiCOT is strikingly different from the reversible, well-defined electrochemical behavior exhibited by films of these polymers.

2. Electrodeposition of poly-sec-butylCOT from THF Solutions

Under specific conditions of solvent and electrolyte, thin films of poly-*sec*-butylCOT could be electrochemically deposited onto electrode surfaces. When predominantly-*trans* poly-*sec*-butylCOT was oxidized in THF-0.1 M $TBABF_4$ (0.5 mg polymer/mL THF), the cathodic return wave indicated that an electroactive material had been deposited onto the electrode. As displayed in Figure 10a, the cathodic peak current obtained under these conditions increased with successive cycling. The reduction of predominantly-*trans* poly-*sec*-butylCOT in CH_2Cl_2-0.1 M $TEABF_4$ produced a similar electrodeposition wave. In both cases, sustained electrochemical cycling produced a thin film of poly-*sec*-butylCOT on the electrode surface.

Even in its neutral form, the electrochemically-deposited predominantly-*trans* poly-*sec*-butylCOT film could not be washed away in pure THF. This may result from a small amount of crosslinking during the electrodeposition process. This is not unexpected in view of the losses in charging capacity that were observed during repetitive cycling of the polymer films. The persistent electroactivity of the deposited film indicated that if crosslinking did occur, it was not sufficient to preclude facile ionic transport through the polymer layer.

Electrodeposited poly-*sec*-butylCOT films exhibited reversible oxidative and reductive doping waves in CH_3CN-0.1 M $TBABF_4$ (Figure 10b). However, the separation between the anodic and cathodic peaks for the oxidative charge/discharge process was extremely small, with E_{pa}-E_{pc} generally less than 50 mV. Nevertheless, the redox potentials for the electrodeposited film were the same as those of cast poly-*sec*-butylCOT films.

Attempts to electrodeposit thick polymer films (> 1 μm) were unsuccessful. For example, the current diminished with time when a constant potential (between 0.45 V and 0.60 V) was maintained in unstirred THF-poly-*sec*-butylCOT solutions. Although this did result in deposition of polymer onto the electrode surface, the films were not uniform in thickness. Additionally, films thicker than 1 μm could not even be produced at a platinum rotating disc electrode (RDE). In this experiment, coulometry (of the discharge wave for the oxidative doping process) at an RDE held at +0.5 V indicated that the film thickness actually diminished with increased rotation rate. Poly-$(CH_3)_3$SiCOT films could not be electrodeposited under any conditions that were explored in this work.

The permeation properties of the thin electrodeposited films were briefly investigated through a few qualitative electrochemical experiments. Glassy carbon electrodes that had been coated with electrodeposited, ≈400±100 nm thick, poly-*sec*-butylCOT films yielded the same peak current and peak potentials for $(CH_3CO)Fc^{+/0}$ in CH_3CN as were observed on a bare glassy carbon electrode. Such behavior is expected because the acetylferrocene$^{+/0}$ redox couple is located at potentials for which the poly-*sec*-butylCOT film is electrically conductive. In contrast, glassy carbon/poly-*sec*-butylCOT electrodes yielded negligible currents for the reduction of benzoquinone to the benzoquinone radical anion. This behavior is expected for a polymer film that was free of gross defects and pinholes, because the benzoquinone$^{0/-}$ redox potential occurs in a range where poly-*sec*-butylCOT films are neutral, and therefore are electrically insulating.

IV. DISCUSSION

A. Substituent Effects on the Doping Potentials and Conjugation Length of Poly-RCOT Materials

The polymerization of substituted cyclooctatetraenes (RCOT) yields unique polyacetylene derivatives. These polymers bear, on the average, one substituent group for every eight carbon atoms in the polymer backbone, but the materials otherwise resemble polyacetylene in stoichiometry. In fact, polyacetylene and the poly-RCOTs share several interesting physical and electronic properties. For example, both types of polymers exhibit chemically reversible *n*-type and *p*-type doping processes, show mid-gap states in the doped films, and undergo *cis-trans* isomerization through doping.

However, unlike polyacetylene, the properties of the poly-RCOTs can be manipulated synthetically. For example, proper choice of the substituent group can yield RCOT polymers that are soluble and are also electrically conductive after doping. In addition, the remarkably sharp and well-defined voltammetric charge/discharge waves of poly-RCOT films[52,53] allow reliable estimates of the thermodynamics for polymer doping.

One of the main goals of our work was to investigate the steric and electronic perturbations possible within the polyRCOT series. The chain twisting of RCOT polymers is primarily determined by the steric bulk of the substituent group; thus, the electronic and electrochemical properties of poly-RCOT films should be strongly influenced by the steric demands of the substituent. This expectation was confirmed by the data for the butyl-substituted poly-RCOTs: as the steric bulk at the point of attachment to the polymer chain increased, the effective conjugation length decreased (R=*n*-butyl, λ_{max}=614 nm; R=*sec*-butyl, λ_{max}=556 nm; R=*tert*-butyl, λ_{max}=432 nm). The separation between $E^{o'}_{ox}$ and $E^{o'}_{red}$ also followed this same trend (Table 1), further confirming the importance of steric effects in these polymers.[54,55]

Inductive effects were also significant in the poly-RCOT materials. Poly-*tert*-butoxyCOT clearly showed an inductive donor substituent effect, because it was more easily oxidized than poly-*n*-butylCOT. Within the series of RCOT polymers with *para*-substituted phenyl substituents,

the steric bulk of the *p*-X-phenyl substituent is constant, so inductive effects should dominate the observed electrochemical and spectroscopic behavior. Consistently, poly-*p*-CF_3-phenylCOT was 0.05 V easier to reduce and 0.04 V more difficult to oxidize than was poly-phenylCOT, and poly *p*-CH_3O-phenyl COT was easier to oxidize and more difficult to reduce than poly-phenylCOT.

Surprisingly, the *tert*-butoxyCOT polymer was also more easily reduced than poly-*n*-butylCOT. In fact, poly-*tert*-butoxyCOT displayed the smallest separation between $E^{o'}_{ox}$ and $E^{o'}_{red}$ of all the poly-RCOT materials studied in this work. An analogous lowering of the band gap has been observed for polythiophenes after substitution with alkoxy groups,[56,57] although the origin of this effect is not well understood.

The optical and electrochemical data can be used together to elucidate some of the more subtle features of the polyRCOT materials. For example, the optical data indicate that poly-$(CH_3)_3$SiCOT has a bulkiness near to the chain that is more similar to poly-*sec*-butylCOT than to poly-*tert*-butylCOT. This is consistent with expectations that the C-Si bond is longer than the C-C bond. Despite the similar optical transition energies for these films, the electrochemical data indicate that $E^{o'}_{ox}$ and $E^{o'}_{red}$ for poly-$(CH_3)_3$SiCOT were shifted significantly positive of $E^{o'}_{ox}$ and $E^{o'}_{red}$ for poly-*sec*-butylCOT. This difference, which cannot be gleaned from the optical data, can be ascribed to the more electropositive nature[58,59] of the $(CH_3)_3Si$ substituent relative to the sec-butyl group.

Although there was a clear variation in redox potentials for the poly-RCOT series, it is useful to put these shifts in perspective with respect to redox shifts that have been observed for other conducting polymers. Specifically, the magnitude of the shifts observed for the poly-RCOT series is small when compared to the substituent effects that have been reported for the 3-substituted thiophene polymers. For example, poly-3-methoxythiophene is more easily oxidized than polythiophene by 0.5 V, [17] and polythiophene is more easily oxidized than poly-3-bromothiophene by 0.25 V.[16] However, comparisons between different types of conjugated polymers must take into account the relative population of the substituent groups on the polymer

chain, and also must consider differences in electronic structure such as delocalization length and bandwidth.

Both optical and electrochemical data indicate that poly-*tert*-butylCOT is significantly less conducting than other poly-RCOTs studied to date. The previous observation[27,34] that poly-*tert*-butylCOT displays neither a weight uptake, nor an increase of electronic conductivity upon exposure to iodine vapor, is understandable in view of the voltammetric results reported herein. For poly-*tert*-butylCOT the oxidation potential is shifted to more positive values than that of poly-*n*-butylCOT or poly-$(CH_3)_3$SiCOT, diminishing the driving force for oxidation of poly-*tert*-butylCOT by I_2(g). Additionally, the irreversibility of the oxidation wave in this system indicates that if a more powerful chemical oxidant were used to oxidize the poly-*tert*-butylCOT film, persistent charge carriers would not be formed. The origin of this chemical instability is not obvious, since poly-*sec*-butylCOT and poly-*n*-butylCOT films are stable in the potential range in which poly-*tert*-butylCOT is irreversibly oxidized.

B. Measurements of Conjugation Length and Doping Stoichiometry

The doping stoichiometry is one of the most desired, yet experimentally elusive properties of conducting polymer films. The difficulty is that as such films are doped, the total conductive area of a polymer-coated electrode increases, and therefore the total electrode capacitance increases. This problem has attracted much debate in the literature,[39-42] but many agree that for such systems the faradaic charge cannot be extracted from the voltammetric data alone.

However, for poly-RCOT films, the sharp, well-defined voltammetry strongly suggests that a discrete amount of faradaic charge flows in a relatively narrow potential range. The spectroelectrochemical data for these films (section **III.A.4**) lends support to this interpretation. Under such conditions, the faradaic charge can be reliably estimated from the voltammetry. As described above, a straightforward analysis of the data yields a ratio of ≈14-15 (C=C)/e for both anodic and cathodic doping.

A check on the validity of this method can be obtained if other, independent determinations of the polymer doping stoichiometry are available. For most poly-RCOT materials, the chain-

carbon to iodine ratio obtained from I_2 weight uptake measurements is 0.11, implying a ratio of 28 chain carbons (*i.e.*, 14 double bonds) per I_3^- counterion. Our estimate from the electrochemical data is in excellent agreement with this value.

The poly-RCOT films also exhibited a discrete second oxidation process. The presence of a discrete second oxidation wave suggests that oxidation beyond the reversible couple for these films occurs as a discrete second step, rather than occurring throughout the plateau region. This chemically irreversible oxidation resulted in a total loss of electroactivity of the polymer film. This "overdoping" possibly produced a gross crosslinking of the polyene segments, resulting in a loss of conjugation in the film. As precedent for this type of reactivity, unsubstituted polyacetylene exhibits a similar, irreversible secondary oxidation step.[61-63]

Even if the over-oxidation region was avoided, the charge capacity of all poly-RCOT films declined significantly after long term potential cycling. Such effects have been commonly observed in the voltammetry of conducting polymer films.[64] This behavior is generally ascribed to charge trapping, although it might also result from chemical instability of the doped films in CH_3CN-[(n-alkyl)$_4$N]$^+$[BF_4]$^-$. We note, however, that the peak potentials, and thus the electronic structure of the bulk poly-RCOT films, remained constant during the loss of charge capacity.

The secondary oxidation potential is relevant to some previously unexplained observations of poly-RCOT doping. For nearly all poly-RCOT films, chemical doping with I_2(g) produces a dramatic increase in electronic conductivity (from $<10^{-8}$ S/cm for the neutral films, to $10\text{-}10^{-2}$ S/cm for I_2(g) doped films). This is consistent with the electrochemical data, because I_2(g) is capable of effecting reversible oxidative doping but is not a strong enough oxidant to promote the destructive over-oxidation step. For poly-*tert*-butoxyCOT, however, I_2(g) is thermodynamically capable of effecting both the reversible doping step and the irreversible over-oxidation process. Thus, the observation that iodine doping does *not* result in high conductivity for poly-*tert*-butoxyCOT, despite a large weight uptake of I_2(g),[27] is nicely explained by the voltammetry.

C. Voltammetry in Solution

Although poly-RCOT films yielded well-defined electrochemical behavior, poly-RCOT/THF solutions yielded poorly defined voltammetry. In fact, such solutions displayed a relatively sharp current onset but never yielded a well-defined limiting current. In solution, the solvated polymer chain can maintain a greater degree of conformational and rotational freedom than in the solid state. The dissolved polymer therefore represents a complex redox system containing multiple, highly coupled redox sites. In such systems, cyclic voltammetry is generally not very informative,[50] and such was the case in our study as well.

A comparison to the voltammetric behavior of *trans*-β-carotene is instructive to understand this behavior. This well-defined 11-ene undergoes a reversible 2-electron oxidation at 0.74 V vs. SCE in CH_2Cl_2, although the resulting dication is known to have a short half-life.[65,66] Under the same conditions that*trans*-β-carotene displayed a reversible 2-electron wave, poly-*sec*-butylCOT and poly-$(CH_3)_3$SiCOT produced the irreversible and broad voltammograms of Figure 8. Therefore, carotene was more difficult to oxidize than these conjugated polymers. However, since *trans*-β-carotene exhibits an oxidation level of 5.5 (C=C)/e^-, by analogy, larger polyenes *in solution* should also display at least this degree of oxidation.

Quantitative information regarding the polymer oxidation level is potentially contained in the steady state current, i_{ss}, obtained in a microelectrode experiment:

$$i_{ss} = 4nFDCr \qquad (1),$$

with F = 96485 coulombs/equiv, D = diffusion coefficient (cm^2/sec), C = concentration (equiv/cm^3), and r= microelectrode radius (cm). However, this method requires an accurate estimate of D. Unfortunately, the nonideal redox response of the dissolved poly-RCOTs precluded a reliable electrochemical determination of D. In addition, constant potential bulk electrolysis experiments were ambiguous, because homogeneous reactions destroyed the oxidized polyene chromophore even at relatively low conversion. However, if poly-*sec*-butylCOT in solution (Figure 9) is assumed to undergo oxidation to the same extent as *trans*-β-carotene (5.5 (C=C)/e^-), then equation (1) yields D= 6.7×10^{-7} cm^2/sec for poly-*sec*-butylCOT. Since this is a reasonable

value for a random coil polymer in a good solvent, the comparison between *trans*-β-carotene and substituted COT polymers in solution may in fact be appropriate. A more precise evaluation of this comparison will, however, only be available when accurate diffusion coefficients can be determined through light scattering experiments or other experimental methods.

D. Poly-RCOT Materials as Substituted Polyacetylenes

In general, there are enough similarities in the optical spectra, electrochemical behavior, and other physical properties that poly-RCOT materials can be considered close approximations to polyacetylene. However, the ability to vary chemically the substituent group in the poly-RCOTs increases the potential significance of this class of materials. In this work, we have exploited some of this synthetic capability to effect desired changes in the solubility and electrochemical properties of these polymers.

The widespread need for processible conducting polymers has hastened the synthesis of a large number of substituted conjugated polymers. In many cases, such as in the family of 3-substituted thiophenes, the substituent group solubilizes the polymer without causing major losses in conductivity. However, soluble, highly conductive polyacetylenes cannot generally be prepared using this approach.[67-69] Typically, materials obtained from the polymerization of substituted acetylenes do not possess the conjugation lengths required to support mobile charge carriers. These short conjugation lengths are a consequence of the steric demands of the bulky substituent groups, which probably induce a twisting in the polyene π-backbone and inhibit effective π-overlap. For this reason, efforts to solubilize polyacetylene have taken other approaches, such as the use of soluble prepolymers that can be converted to polyacetylene in a single, high yield step.[70,71] An alternative strategy has been to solubilize polyacetylene segments using block and graft copolymers.[72-74] However, these materials also lack many of the desired physical properties of soluble conducting polymer phases.

Notably, the transition metal catalyzed ROMP of substituted cyclooctatetraene derivatives provides a liquid phase route to polyacetylene-like materials. As shown herein, the solubility and electronic properties of these polymers can be altered by the selection of various substituent

groups. Despite the increased synthetic flexibility of this route, there is still a need to incorporate additional functionality onto the polyacetylene backbone. For example, of the polymers listed in Table 1, only poly-*sec*-butylCOT, poly-$(CH_3)_3$SiCOT, and poly-*tert*-butylCOT were truly soluble in the predominantly-*trans* configuration. Other poly-RCOT materials were soluble immediately after synthesis, however, they spontaneously isomerized to the thermodynamically stable form and then formed aggregates. Thus, these materials could only be studied reproducibly as thin films. The variation of the substituent group is presently constrained by the existing ROMP catalysts, but this limitation may soon be surmounted by the availability of newer, more selective catalysts. This should allow the incorporation of even more diverse functionality, and should allow exploitation of this class of conducting polymers in an even wider range of chemical, physical, and electrochemical applications.

V. CONCLUSIONS

The ROMP of substituted COT monomers results in a family of high molecular weight substituted polyenes. These materials have many similarities to polyacetylene, including the presence of reversible redox processes for oxidative and reductive doping, the formation of mid-gap transitions in doped films, and the presence of facile, electrochemically induced *cis-trans* isomerization processes. However, the ability to vary the substituent group in the poly-RCOTs increases the potential significance of this class of materials. The substituent group exerts a significant influence on the electronic and electrochemical properties of these materials; furthermore, we have found that such effects can generally be predicted from the steric and electronic properties of the substituent group. This provides an impetus for the synthesis of RCOT polymers that are substituted with more strongly perturbing polar groups, and establishes a benchmark for future improvements in this class of polyenes.

VI. ACKNOWLEDGMENTS

We acknowledge the Office of Naval Research (RHG) and the National Science Foundation (NSL, grant CHE-8814694; RHG and NSL joint grant CHE-9202583) for support of this work. We also wish to thank the IBM Corp. (EJG), the American Chemical Society Division

of Organic Chemistry (CBG), and Smith Kline&French Laboratories (CGB) for research fellowships. We also thank Prof. F.C. Anson for helpful discussions, and thank the reviewers for suggestions regarding the possible effects of Fermi level shifts on the absorption spectra of the polyenes.

VII. REFERENCES

(1) Gorman, C. B.; Grubbs, R. H. In *Conjugated Polymers: The Novel Science and Technology of Highly Conducting and Nonlinear Optically Active Materials*; J. L. Bredas and R. Silbey, Eds.; Kluwer: Boston, 1991; pp. 1-48.

(2) Reynolds, J. L.; Baker, C. K.; Jolly, C. A.; Poropatic, P. A.; Ruiz, J. P. In *Conductive Polymers and Plastics*; J. M. Margolis, Ed.; Chapman and Hall: New York, 1989.

(3) *Electrochemistry of Conducting Polymers*; Plocharski, J.; Roth, S., Eds.; Trans Tech Publications: Switzerland, 1989; Vol. 42.

(4) Patil, A. O.; Ikenoue, Y.; Wudl, F.; Heeger, A. J. *J. Am. Chem. Soc.* **1987**, *109*, 1858-1859.

(5) Rughooputh, S. D. D. V.; Nowak, M.; Heeger, A. J.; Wudl, F. *Synth. Met.* **1987**, *21*, 41-50.

(6) Askari, S. H.; Rughooputh, S. D. D. V.; Wudl, F. *Synth. Met.* **1989**, *29*, E129-E134.

(7) Burroughes, J. H.; Bradley, D. D. C.; Brown, A. R.; Marks, R. N.; MacKay, K. D.; Friend, R. H.; Burn, P. L.; Holmes, A. B. *Nature* **1990**, *347*, 539-541.

(8) Burroughes, J. H.; Jones, C. A.; Friend, R. H. *Synth. Met.* **1989**, *28*, C735-C745.

(9) Horowitz, G. *Adv. Mater.* **1990**, *2*, 287-292.

(10) Wöhrle, D.; Meissner, D. *Adv. Mater.* **1991**, *3*, 129-138.

(11) Sailor, M. J.; Ginsburg, E. J.; Gorman, C. B.; Kumar, A.; Grubbs, R. H.; Lewis, N. S. *Science* **1990**, *249*, 1146-1149.

(12) Sailor, M. J.; Klavetter, F. L.; Grubbs, R. H.; Lewis, N. S. *Nature* **1990**, *346*, 155.

(13) Kanicki, J. In *Handbook of Conducting Polymers*; T. J. Skotheim, Ed.; Dekker: New York, 1986; Vol. 1; pp 543-660.

(14) Waltman, R. J.; Bargon, J.; Diaz, A. F. *J. Phys. Chem.* **1983**, *87*, 1459-1463.

(15) Patil, A. O. *Synth. Met.* **1989**, *28*, C495-C500.

(16) Tourillon, G.; Garnier, F. *J. Electroanal. Chem.* **1984**, *161*, 51-58.

(17) Kaeriyama, K.; Tanaka, S.; Sato, M.; Hamada, K. *Synth. Met.* **1989**, *28*, C611-C620.

(18) Masuda, T.; Higashimura, T. *Adv. Polym. Sci.* **1986**, *81*, 121.

(19) Gibson, H. W. In *Handbook of Conducting Polymers*; T. J. Skotheim, Ed.; Dekker: New York, 1986; Vol. 1; Ch.11.

(20) Chien, J. C. W. *Polyacetylene*; Academic Press: Orlando, Fl., 1984.

(21) Ginsburg, E. J.; Gorman, C. B.; Marder, S. R.; Grubbs, R. H. *J. Am. Chem. Soc.* **1989**, *111*, 7621-7622.

(22) Ginsburg, E. J.; Gorman, C. B.; Grubbs, R. H.; Klavetter, F. L.; Lewis, N. S.; Marder, S. R.; Perry, J. W.; Sailor, M. J. In *Conjugated Polymeric Materials: Opportunities in Electronics, Optoelectronics, and Molecular Electronics*; J. L. Bredas and R. R. Chance, Eds.; Kluwer Academic Publishers: The Netherlands, 1990; pp 65-81.

(23) Gorman, C. B.; Ginsburg, E. J.; Marder, S. R.; Grubbs, R. H. *Angew. Chem. Adv. Mater.* **1989**, *101*, 1603-1606.

(24) Gorman, C. B.; Ginsburg, E. J.; Moore, J. S.; Jozefiak, T. J.; Lewis, N. S.; Grubbs, R. H.; Marder, S. R.; Perry, J. W. *Synth. Met.* **1991**, *41*, 1033.

(25) Marder, S. R.; Perry, J. W.; Klavetter, F.; Grubbs, R. H. *Chem. Mater.* **1989**, *1*, 171-173.

(26) Moore, J. S.; Gorman, C. B.; Grubbs, R. H. *J. Am. Chem. Soc.* **1991**, *113*, 1704-1712.

(27) Gorman, C. B. Ph. D. Thesis, California Institute of Technology, 1991.

(28) Viallat, A.; Rossi, G. *J. Chem. Phys.* **1990**, *92*, 4548-4556.

(29) Spiegel, D.; Pincus, P.; Heeger, A. J. *Synth. Met.* **1989**, *28*, C385-C391.

(30) Spiegel, D. R. *Macromolecules* **1991**, *24*, 3568-3572.

(31) Pincus, P. A.; Rossi, G.; Cates, M. E. *Europhys. Lett.* **1987**, *4*, 41-46.

(32) Nowak, M. J.; Rughooputh, S. D. D. V.; Hotta, S.; Heeger, A. J. *Macromolecules* **1987**, *20*, 965-968.

(33) Patil, A. O.; Heeger, A. J.; Wudl, F. *Chem. Rev.* **1988**, 183-200.

(34) Ginsburg, E. J. Ph. D. Thesis, California Institute of Technology, 1991.

(35) Johnson, L. K.; Virgil, S. C.; Grubbs, R. H. *J. Am. Chem. Soc.* **1990**, *112*, 5384-5385

(36) *Handbook of Conducting Polymers*; Skotheim, T. A., Ed.; Marcel Dekker: New York, 1986; Vol. 1 and 2.

(37) Heinze, J.; Mortensen, J.; Hinkelmann, K. *Synth. Met.* **1987**, *21*, 209-214.

(38) Heinze, J. *Synth. Met.* **1991**, *41-43*, 2805-2823.

(39) Meerholz, K.; Heinze, J. *Angew. Chem. Int. Ed. Engl.* **1990**, *29*, 692-695.

(40) Cai, Z.; Martin, C. R. *J. Electroanal. Chem.* **1991**, *300*, 35-50.

(41) Feldberg, S. W. *J. Am. Chem. Soc.* **1984**, *106*, 4671-4674.

(42) Tanguy, J.; Pron´, A.; Zagórska, M.; Kulszewicz-Bajer, I. *Synth. Met.* **1991**, *45*, 81-105.

(43) MacDiarmid, A. G.; Kaner, R. B. In *Handbook of Conducting Polymers*; T. J. Skotheim, Ed.; Dekker: New York, 1986; Vol. 1; p. 692.

(44) Pekker, S.; Jánossy, A. In *Handbook of Conducting Polymers*; T. J. Skotheim, Ed.; Derkker: New York, 1986; Vol. 1; pp 48-49.

(45) Kaneto, K.; Maxfield, M.; Nairns, D. P.; MacDiarmid, A. G.; Heeger, A. J. *J. Chem. Soc. Faraday Trans. 1* **1982**, *78*, 3417-3429.

(46) Maxfield, M.; Mu, S. L.; MacDiarmid, A. G. *J. Electrochem. Soc.* **1985**, *132*, 838-841.

(47) Feldblum, A.; Heeger, A. J.; Chung, T.-C.; MacDiarmid, A. G. *J. Chem. Phys.* **1982**, *77*, 5114-5121.

(48) Heinze, J.; Bilger, R.; Meerholz, K. *Ber. Bunsenges. Phys. Chem.* **1988**, *92*, 1266-1271.

(49) LeBlevenec, L. F.; Gaudiello, J. G. *J. Electroanal. Chem.* **1991**, *312*, 97-114.

(50) Gale, D. C.; Gaudiello, J. G. *J. Am. Chem. Soc.* **1991**, *113*, 1610-1618.

(51) Cain, S. R.; Gale, D. C.; Gaudiello, J. G. *J. Phys. Chem.* **1991**, *95*, 9584-9589.

(52) Nigrey, P. J.; MacDiarmid, A. G.; Heeger, A. J. *Mol. Cryst. Liq. Cryst.* **1982**, *83*, 309.

(53) Diaz, A. F.; Clarke, T. C. *J. Electroanal. Chem.* **1980**, *111*, 115-117.

(54) The difference between formal potentials for the oxidative and reductive doping processes, however, should not be equated with the polymer bandgap, since an electrochemical determination

of the band gap of polymer films requires measurement of threshold potentials for the injection and ejection of charge under conditions close to thermodynamic equilibrium.

(55) Kaner, R. B.; Porter, S. J.; Nairns, D. P.; MacDiarmid, A. G. *J. Chem. Phys.* **1989**, *90*, 5102-5107.

(56) Feldhues, M.; Kaempf, G.; Litterer, H.; Mecklenburg, T.; Wegener, P. *Synth. Met.* **1989**, *28*, C487-C493.

(57) LeClerc, M.; Daoust, G. *Synth. Met.* **1991**, *41*, 529-532.

(58) Paquette, L. A.; Wright III, C. D.; Traynor, S. G.; Taggart, D. L.; Ewing, G. D. *Tetrahedron* **1976**, *32*, 1885-1891.

(59) Giordan, J. C.; Moore, J. H. *J. Am. Chem. Soc.* **1983**, *105*, 6541.

(60) Shacklette, L., W.; Toth, J. E.; Murthy, N. S.; Baughman, R. H. *J. Electrochem. Soc.* **1985**, *132*, 1529-1535.

(61) Krische, B.; Zagorska, M. *Synth. Met.* **1989**, *28*, 257-262.

(62) Chien, J. C. W.; Schlenoff, J. B. *Nature* **1984**, *311-363*, 362.

(63) Note that in some media, the second oxidation process does not result in a loss of electroactivity for the polymer film: Ofer, D.; Park, L. Y.; Schrock, R. R.; Wrighton, M. S. *Chem. Mater.* **1991**, *3*, 573-575.

(64) Borjas, R.; Buttry, D. A. *Chem. Mater.* **1991**, *3*, 872-878.

(65) Khaled, M.; Hadjipetrou, A.; Kispert, L. *J. Am. Chem. Soc.* **1990**, *94*, 5164-5169.

(66) Grant, J. L.; Kramer, V. J.; Ding, R.; Kispert, L. D. *J. Am. Chem. Soc.* **1988**, *110*, 2151-2157.

(67) Yamaguchi, M.; Torisu, K.; Hiraki, K.; Minami, T. *Chem. Lett.* **1990**, 2221-2222.

(68) Subramanyam, S.; Blumstein, A. *Macromolecules* **1991**, *24*, 2668-2674.

(69) Kang, E. T.; Neoh, K. G.; Masuda, T.; Higashimura, T.; Yamamoto, M. *Polymer* **1989**, *30*, 1328-1331.

Edwards, J. H.; Feast, J. W. *Polymer* **1980**, *21*, 595-596.

(71) Swager, T. M.; Grubbs, R. H. *J. Am. Chem. Soc.* **1989**, *111*, 4413-4422.

(72) Stelzer, F.; Grubbs, R. H.; Leising, G. *Polymer* **1991**, *32*, 1851-1856.

(73) Baker, G. L.; Bates, F. S. *Macromolecules* **1984**, *17*, 2619-2626.

(74) Stowell, J. A.; Amass, S. J.; Beevers, M. S.; Farren, T. R. *Polymer* **1989**, *30*, 195-201.

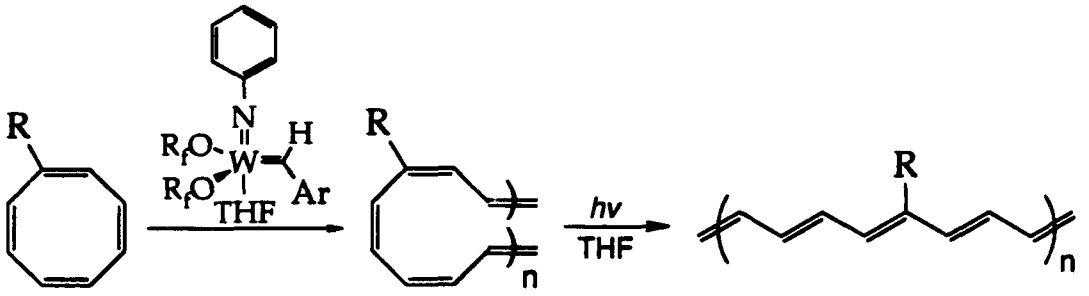

Scheme 1. The ROMP synthesis of poly-RCOTs (R = alkyl, p-X-phenyl, t-butoxy, $(CH_3)_3Si$) from cyclooctatetraene derivatives, using a well-defined tungsten alkylidene metathesis catalyst ($R_fO = OC(CF_3)_2CH_3$, Ar = *o*-methoxyphenyl).

TABLE 1. Potentials for Oxidation and Reduction of poly-RCOT Films.

poly-RCOT	$E^{o'}_{ox}$[a]	$E^{o'}_{red}$[a]	$E^{o'}_{ox} - E^{o'}_{red}$	λ_{max}(nm) solution[b]
n-butyl	0.39	-1.39	1.78	615[d]
sec-butyl	0.42	-1.38	1.80	556
tert-butyl	0.58[c]	-1.56	2.14	432
tert-butoxy	0.30	-1.35	1.66	594[d]
trimethylsilyl	0.52	-1.27	1.79	540
p-CH_3O-Ph	0.44	-1.33	1.77	>600[d]
Ph	0.45	-1.24	1.69	≈620[d]
p-CF_3-Ph	0.49	-1.19	1.68	>600[d]

[a]Potential±0.005 V vs. SCE, determined as: $((E_{pa}+E_{pc})/2)$ from voltammograms of polymer films on a glassy carbon electrode in CH_3CN-0.1 M $TMABF_4$. In each case, E_{pa}-E_{pc} was <100mV. $E^{o'}_{ox}$ refers to the formal potential for the oxidative doping process of the neutral polymer film, while $E^{o'}_{red}$ refers to the reductive doping process of the neutral film. [b]Spectra measured in THF solution, taken from reference 27. [c]This is the potential of the maximum anodic current in the irreversible oxidation of the polymer film. [d]Solutions of these polymers were not homogeneous (see text).

TABLE 2. Energy of Absorbance Maxima For Neutral and Doped Polymer Films.

polymer	neutral (eV)	oxidized (eV)	reduced (eV)
poly-$(CH_3)_3$SiCOT	2.3	0.88-0.96	0.9-1.0
poly-*sec*-butylCOT	2.3	0.80-0.90	0.81-0.87
polyacetylene[a]	2.0	0.65-0.75	0.65-0.75

[a]From Reference 33.

FIGURE CAPTIONS

Figure 1. Cyclic voltammogram (20 mV/sec) of a poly-*sec*-butylCOT film (4.7×10^{-6} g) on a glassy carbon electrode (0.24 cm^2 area) in CH_3CN-0.1 M $TMABF_4$. Arrowhead indicates inital scan direction.

Figure 2. Current vs. potential (thick line, left ordinate) and charge vs. potential (thin line, right ordinate) voltammograms at 20 mV/sec for a poly-*sec*-butylCOT film (1.9×10^{-6} g) on a glassy carbon electrode (0.24 cm^2 area) in CH_3CN-0.1 M $TMABF_4$. The dashed line shows the calculated faradaic charge vs. potential (see text).

Figure 3. Cyclic voltammogram (20 mV/sec) of a poly-*sec*-butylCOT film (1.9×10^{-6} g) on a glassy carbon electrode (0.24 cm^2 area) in CH_3CN-0.1 M $TMABF_4$. Arrowhead indicates inital scan direction. The second cycle shows the loss of electroactivity resulting from scanning through the second oxidation wave.

Figure 4. Visible-near-IR spectra of a poly-*sec*-butylCOT film on an In_2O_3 electrode coated onto a glass slide. Solid line: neutral film, dashed line: oxidized film, dotted line: reduced film. The spectroelectrochemistry was performed in CH_3CN-0.1 M $TEABF_4$. In several independent experiments, neutral poly-COT films showed no absorbance in the near infrared region of the spectrum.

Figure 5. Visible spectra of a poly-*sec*-butylCOT film during incremental oxidation from 0.30 V to 0.54 V in CH_3CN-0.1 M $TBABF_4$. The first and last steps were each 60 mV, and all other steps were 30 mV. The spectra were collected using an In_2O_3 electrode that had been coated onto a glass slide.

Figure 6. Cyclic voltammetry (50 mV/sec) of a predominantly-*cis* configuration poly-*sec*-butylCOT film (1.3×10^{-6} g) on a glassy carbon electrode (0.24 cm^2 area) in CH_3CN-0.1 M $TBABF_4$. Arrowhead indicates scan direction on the initial sweep. The first oxidation sweep consumed 5.0×10^{-4} coulombs of charge, while the second oxidation sweep consumed 4.5×10^{-4} coulombs.

Figure 7. TOP: Cyclic voltammogram (50 mV/sec) of predominantly-*cis* configuration poly-*sec*-butylCOT film ($1.0x10^{-6}$ g) on a glassy carbon electrode (0.24 cm^2 area) in CH_3CN-0.1 M $TBABF_4$. Arrowhead indicates scan direction on the initial sweep. The first oxidation sweep to +780 mV (resulting in isomerization) consumed $3.9x10^{-4}$ coulombs of charge, and the second oxidation sweep to +530 mV consumed $2.4x10^{-4}$ coulombs . BOTTOM: Cyclic voltammogram (50 mV/sec) of an equivalent predominantly-*cis* configuration poly-*sec*-butylCOT film ($1.0x10^{-6}$ g). The first oxidation sweep to +580 mV (resulting in incomplete isomerization) consumed $8.5x10^{-5}$ coulombs . The second oxidation sweep to +530 mV consumed $6.7x10^{-5}$ coulombs .

Figure 8. Cyclic voltammetry (20 mV/sec) of a poly-*sec*-butylCOT (0.5 mg/ml) solution in CH_2Cl_2-0.1 M $TBABF_4$. The voltammetry was performed using a platinum electrode with an area of 0.026 cm^2.

Figure 9. Microelectrode voltammetry (20 mV/sec) of a poly-*sec*-butylCOT (0.3 mg/ml) solution in CH_2Cl_2-0.1 M $TBABF_4$. The voltammetry was performed using a platinum microelectrode with a radius of 4.23 μm.

Figure 10. TOP: Cyclic voltammogram (50 mV/sec) of a poly-*sec*-butylCOT (0.5 mg/ml) solution in THF-0.1 M $TBABF_4$ at a glassy carbon electrode (0.24 cm^2 area). Arrowhead indicates direction of the first sweep. BOTTOM: Cyclic voltammogram (50 mV/sec) of the resulting polymer modified electrode in CH_3CN-0.1 M $TBABF_4$.

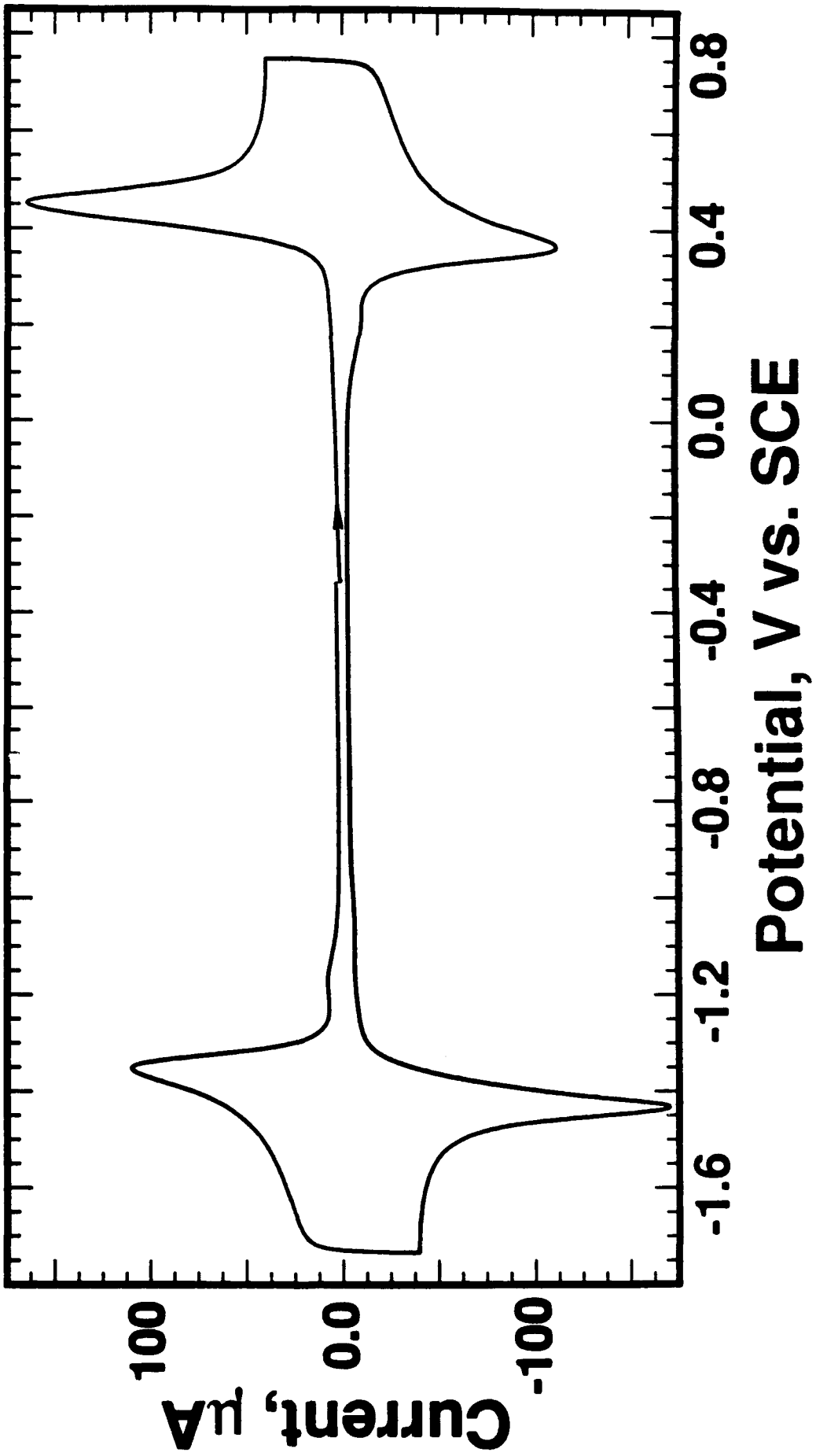

Figure 1

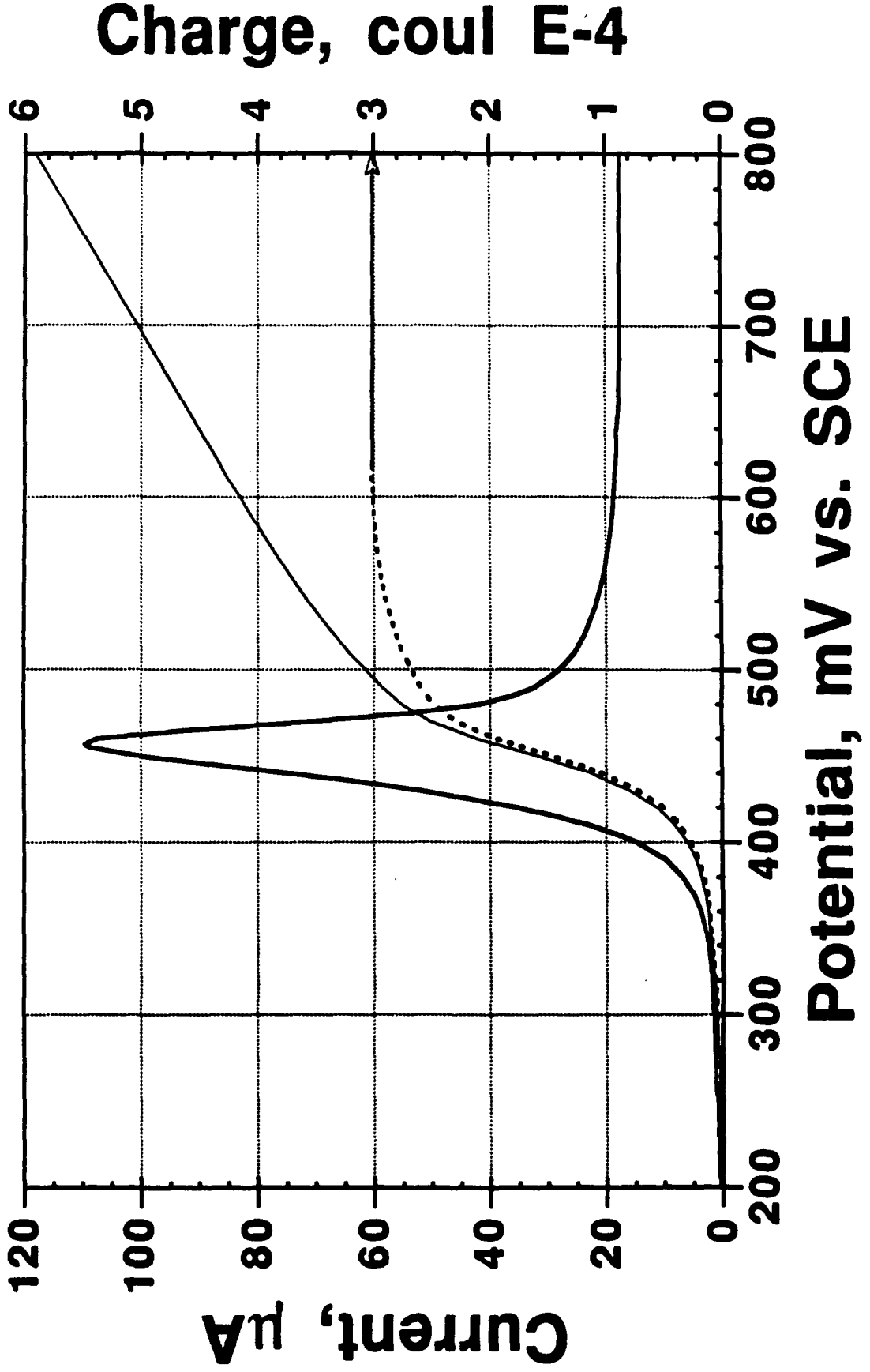
Charge, coul E-4
6
5
4
3
2
1
0
800
700
600
500
400
300
200
Potential, mV vs. SCE
120
100
80
60
40
20
0
Current, μA

Figure 2

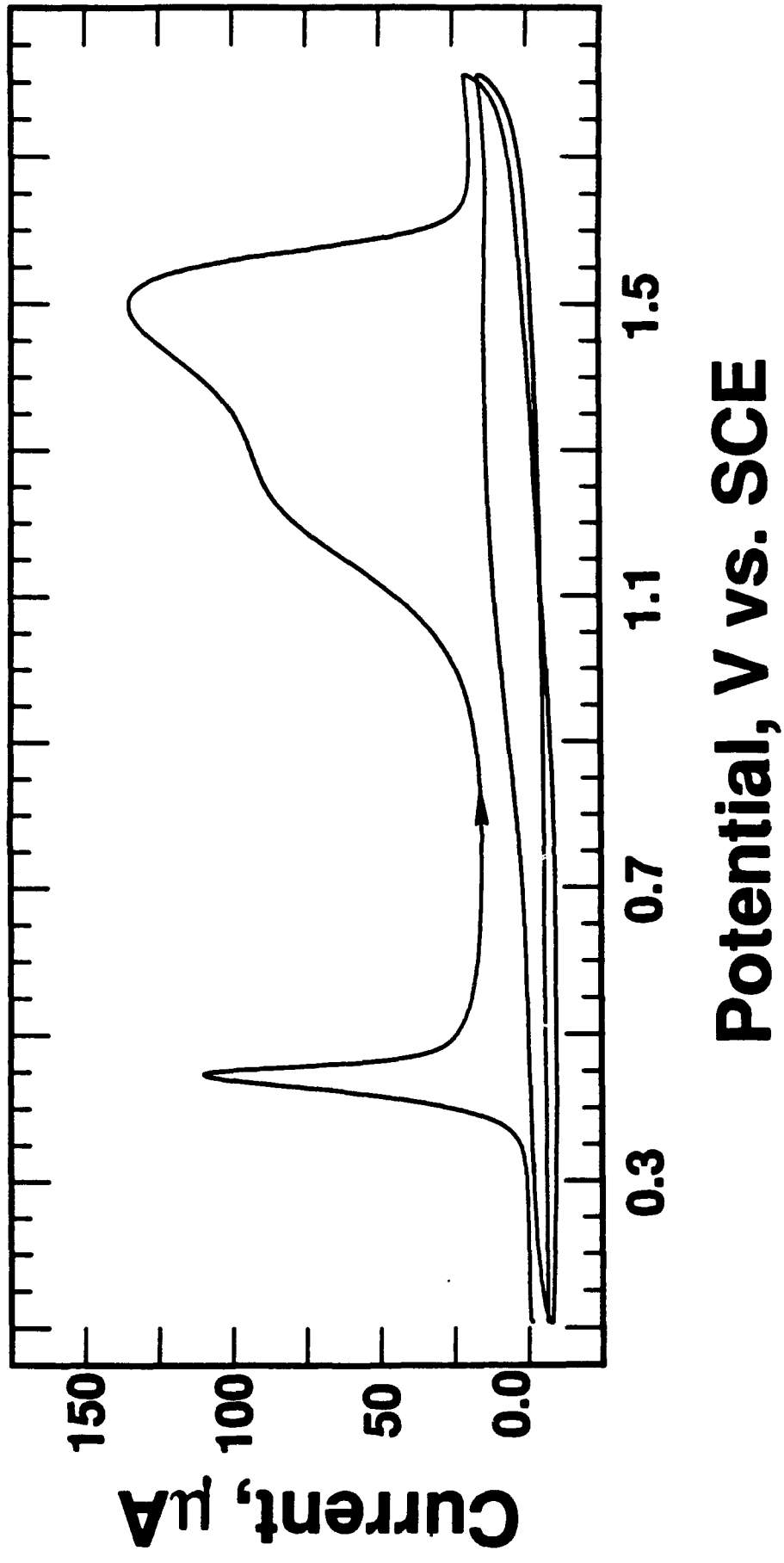

Figure 3

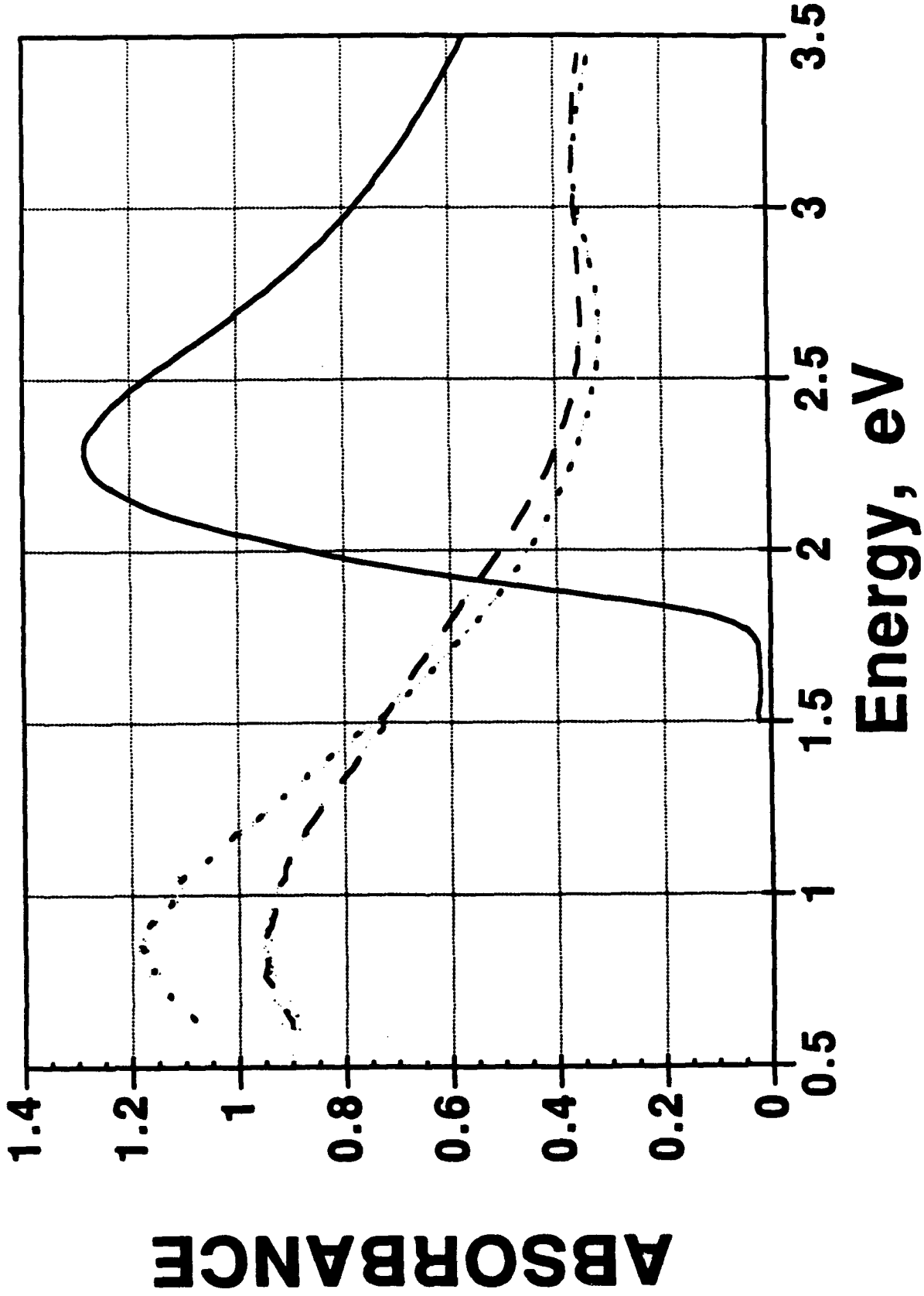

Figure 4

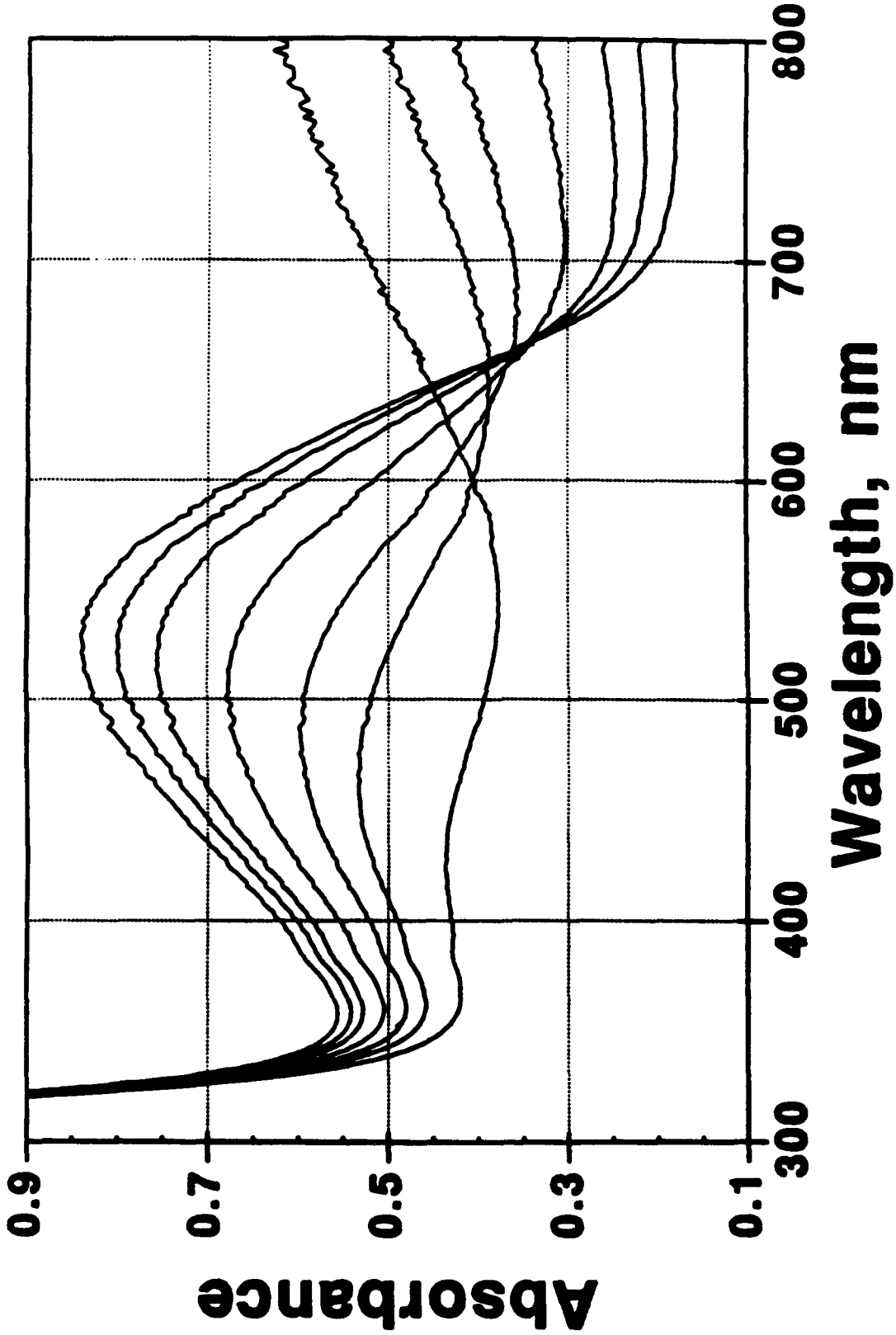
Absorbance
0.9
0.7
0.5
0.3
0.1
300
400
500
600
700
800
Wavelength, nm

Figure 5

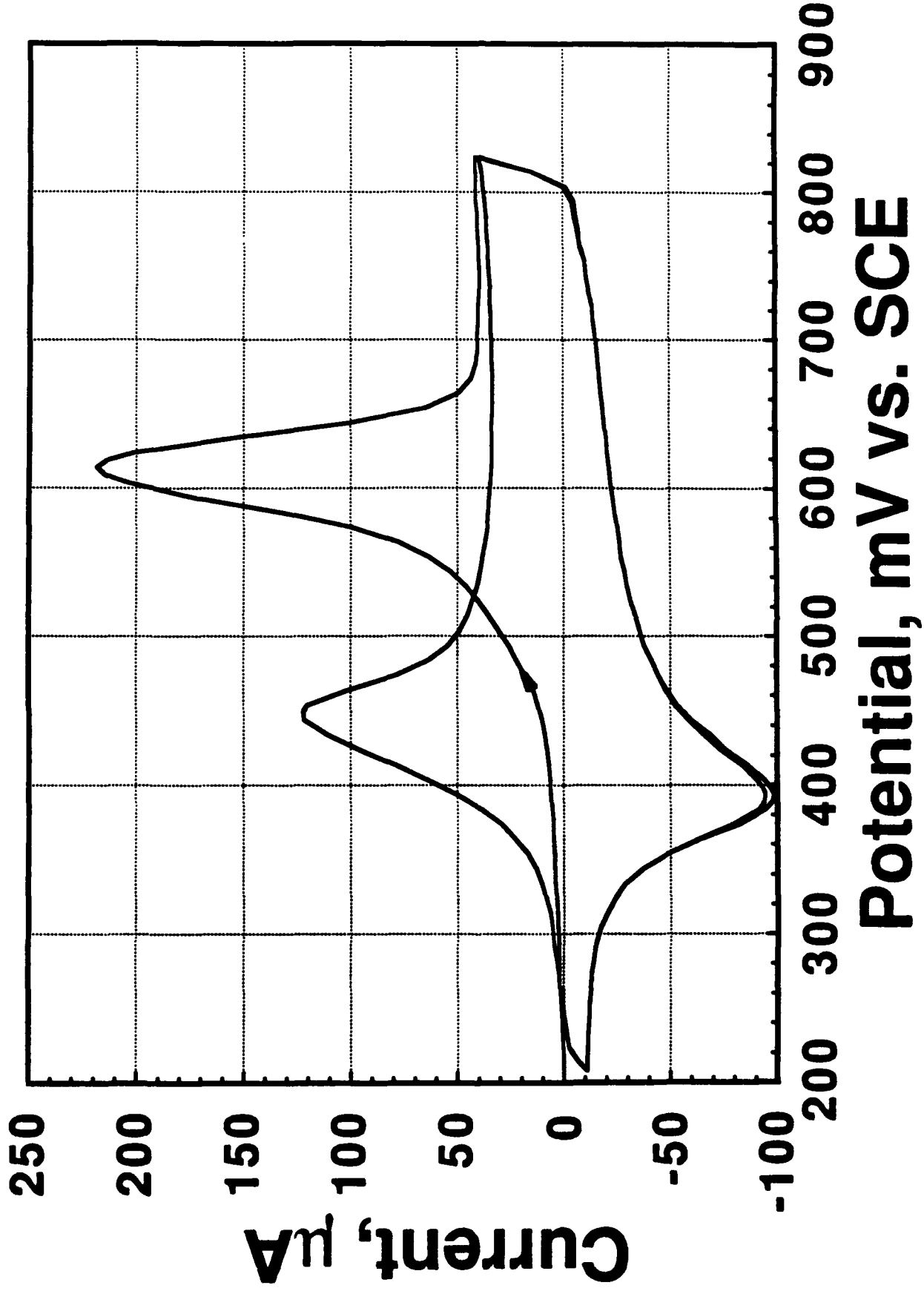
Current, μA
250
200
150
100
50
0
-50
-100
Potential, mV vs. SCE
200
300
400
500
600
700
800
900

Figure 6

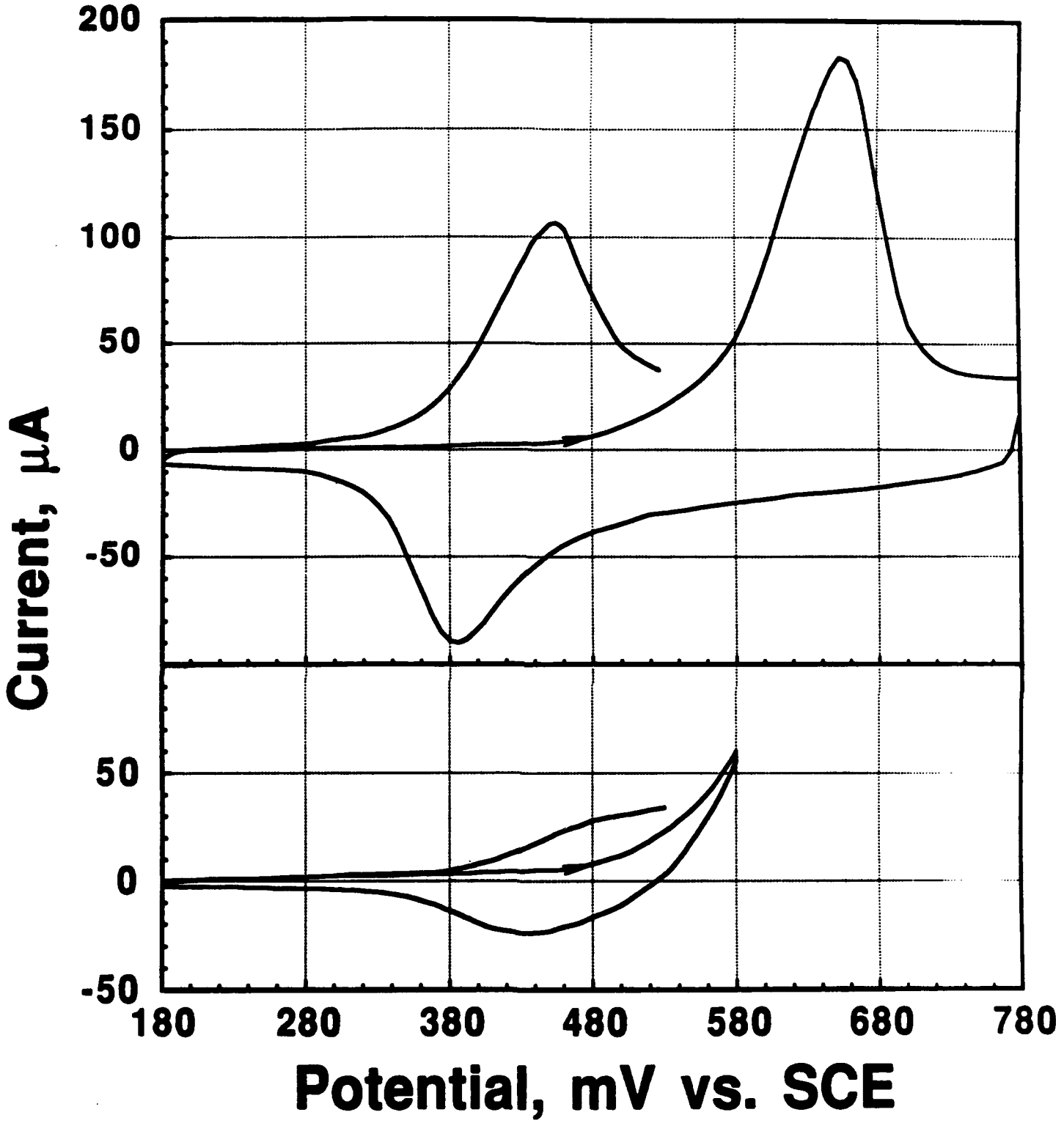
200
150
100
50
0
-50
50
0
-50
Current, µA
180
280
380
480
580
680
780
Potential, mV vs. SCE

Figure 7

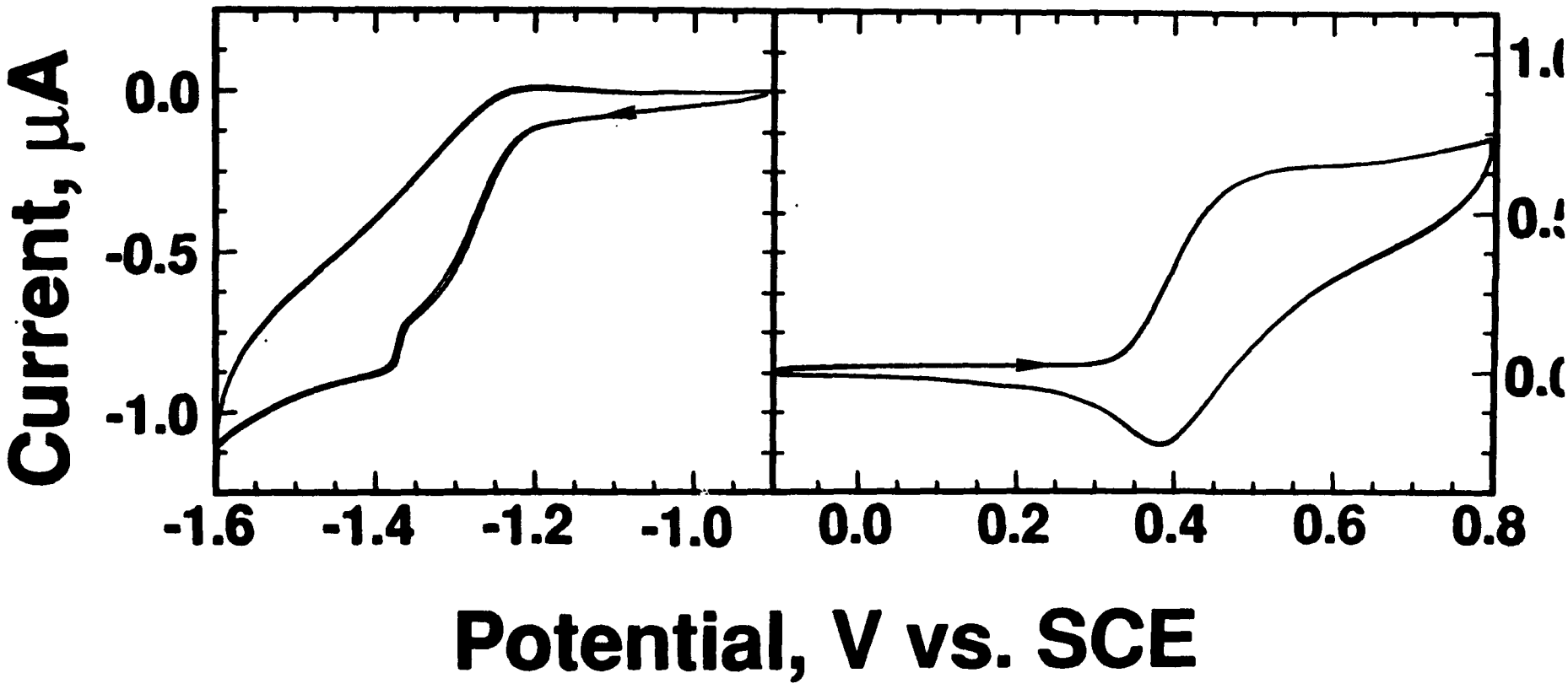

Figure 8
42

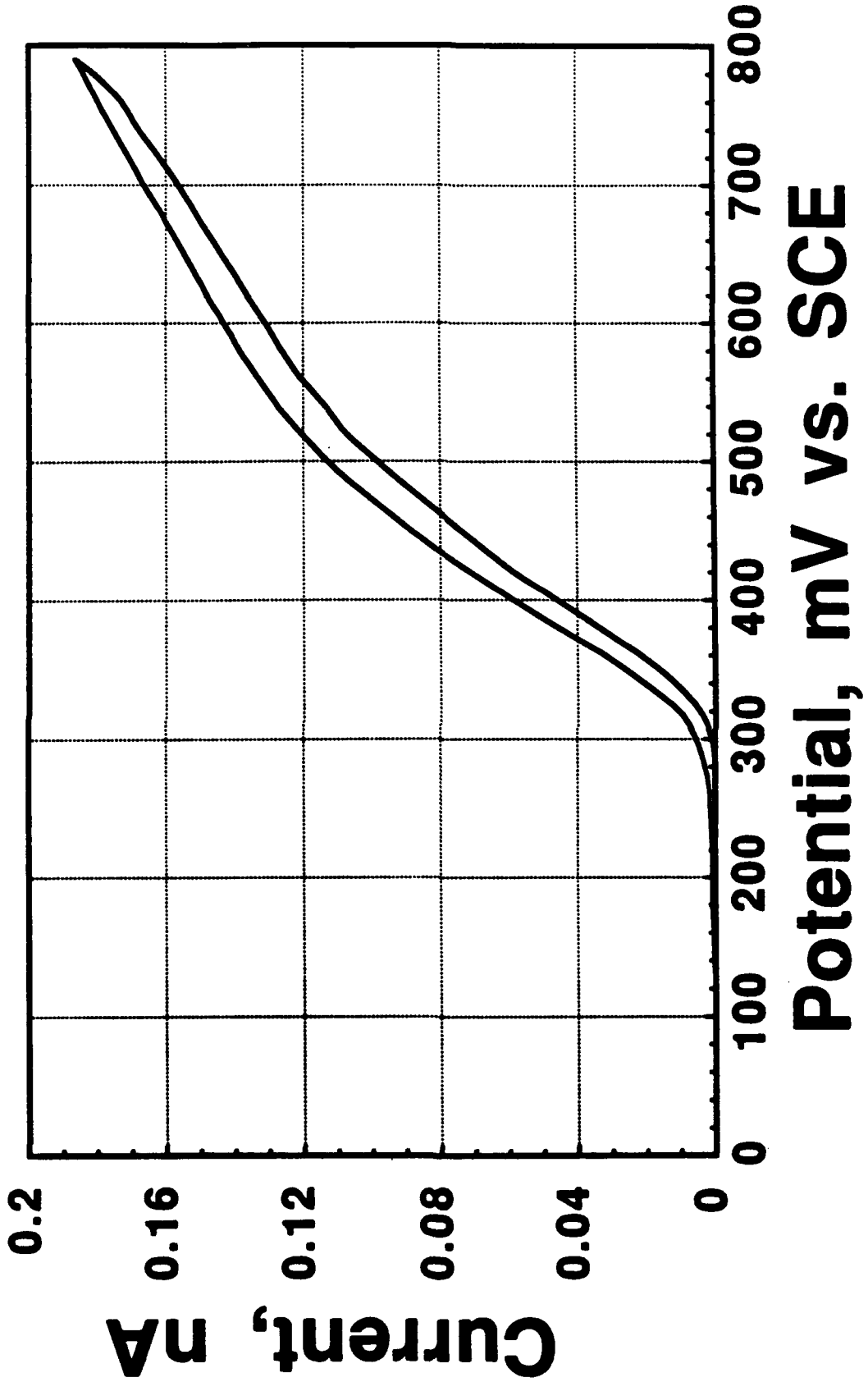
Current, nA
0.2
0.16
0.12
0.08
0.04
0
0
100
200
300
400
500
600
700
800
Potential, mV vs. SCE

Figure 9

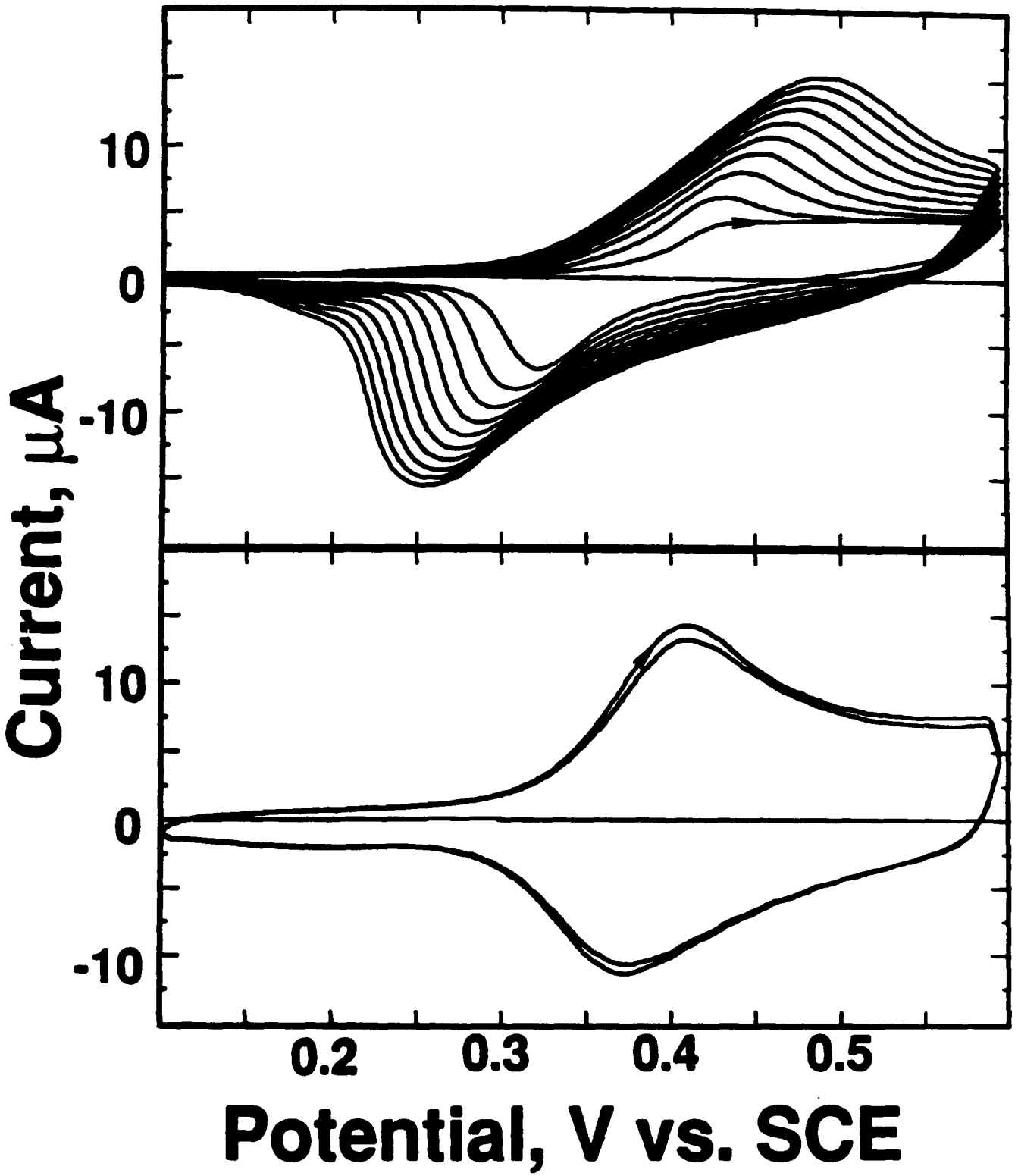

Figure 10